Mineralogical Magazine, April 2001, Vol. 65(2), pp. 221–248

Monte Carlo methods for the study of cation ordering in minerals

M. C. WARREN[1,2], M. T. DOVE[1,*†], E. R. MYERS[1,3], A. BOSENICK[1,4], E. J. PALIN[1], C. I. SAINZ-DIAZ[5], B. S. GUITON[1] AND S. A. T. REDFERN[1]

[1] Department of Earth Sciences, University of Cambridge, Downing Street, Cambridge CB2 3EQ, UK
[2] Present address: Department of Earth Sciences, The University of Manchester, Manchester M13 9PL, UK
[3] Present address: Department of Pure Mathematics and Mathematical Statistics, University of Cambridge, 16 Mill Lane, Cambridge CB2 1SB, UK
[4] Present address: Martenshofweg 9, 24109 Kiel, Germany
[5] Estacion Experimental del Zaidin, CSIC, C/ Profesor Albareda, 1, 18008-Granada, Spain

ABSTRACT

This paper reviews recent applications of Monte Carlo methods for the study of cation ordering in minerals. We describe the program Ossia99, designed for the simulation of complex ordering processes and for use on parallel computers. A number of applications for the study of long-range and short-range order are described, including the use of the Monte Carlo methods to compute quantities measured in an NMR experiment. The method of thermodynamic integration for the determination of the free energy is described in some detail, and several applications of the method to determine the thermodynamics of disordered systems are outlined.

KEYWORDS: Monte Carlo simulation, cation ordering, NMR, phase transitions, aluminosilicates.

Introduction

THE Monte Carlo (MC) method was invented as a tool to generate configurations of a system from which to calculate thermodynamic averages. It is an ideal tool for the computational study of ordering processes in solids when the energy of a configuration can be described by a model Hamiltonian. The MC method, which is described in detail in the following section, is simple to implement, but extremely powerful in that it allows the generation of many configurations of a sample from which thermodynamic averages can be calculated.

In this paper we describe the implementation of a MC strategy for the simulation of cation ordering in minerals, which is based on the use of model interactions as discussed in the previous paper (Bosenick *et al.*, 2001*a*), and which has been used in a wide variety of applications (Thayaparam *et al.*, 1994, 1996; Dove, 1999; Dove *et al.*, 1996, 2000; Bosenick *et al.*, 2000; Warren *et al.*, 2000*a,b*). In fact, the basic equations and their implementation are appropriate for any system with atomic ordering, including metal alloys and ceramic oxides. However, in this paper we are particularly motivated by ordering processes such as the ordering of Al/Si cations on tetrahedral sites or Mg/Al cations on octahedral sites, and even more complicated ordering processes. Thus the basic Hamiltonian expressions and analysis tools discussed in this paper are those most appropriate for these types of ordering processes. The MC method can be used for the study of systems with ordering phase transitions, solid solutions in which there is no long-range order, and non-convergent ordering processes. The MC method will give information about both long-range and short-range order. We describe here a number of examples of the use of the MC method for studies of a wide range of ordering processes.

* E-mail: martin@esc.cam.ac.uk
† Corresponding author

One of the purposes of this paper is to describe the details of an implementation of the MC method for massively parallel processor (MPP) machines. These are computers that contain many separate processors, and which therefore can perform many calculations in parallel. There are several ways in which a simulation procedure can be parallelized for MPP machines, because there are usually several parallel aspects to the problem. Some of these are inherent to the simulation method, and some to the scientific applications using the methods. We will discuss these issues with respect to the implementation for MPP.

The discussion of the MC method as applied to the study of cation ordering is developed following specific approaches, with a common set of examples linking the separate aspects of the discussions. In the next section we describe the MC method, its application to the study of cation ordering processes, and our implementation using MPP machines. We then discuss the use of MC methods to study long-range order, followed by a discussion of calculations of short-range order and the link to NMR experiments. The third area of discussion is the application of thermodynamic integration methods to determine thermodynamic properties.

The Monte Carlo method

The basics of the Monte Carlo method

The simplest implementation of the MC method is for a system containing spins that point up or down, which are represented by the variable σ with values +1 and −1 respectively. Consider the case of a simple antiferromagnetic Ising Hamiltonian,

$$H = J\sum_{\langle i,j\rangle}\sigma_i\sigma_j$$

where the angle brackets are used to denote that the sum is over all relevant pairs of neighbouring spins i and j. At zero temperature, if $J > 0$, the lowest energy state has neighbouring spins of opposite value, giving the most negative energy allowed. On heating, the entropic term in the free energy allows some of the spin values to change sign, and eventually at a temperature above a critical temperature all spins have equal probability of having each of the two possible values. There is no analytic expression for the free energy of this Hamiltonian in three dimensions, and in a case like this the MC method provides a computational method to study the behaviour of the Hamiltonian. We will discuss later how the case of cation ordering can be represented by a Hamiltonian that is very similar to the Ising Hamiltonian, with the spin variables being used to define the occupancy of a given site.

The MC procedure is relatively straightforward in principle (Yeomans, 1992). We consider a sample containing many spins with a Hamiltonian of the form of the Ising model, and we are interested in the behaviour at temperature T. Suppose that a possible change in the system causes an energy change $E \rightarrow E + \Delta E$. In the MC method a change in the configuration is proposed at random. For the Ising model, this will correspond to changing the sign of a spin chosen at random. If the energy change is negative or zero, the change is accepted. On the other hand, if the change in energy is positive, the change is accepted with probability

$$P(E \rightarrow E + \Delta E) = \exp(-\beta\Delta E)$$

where $\beta = 1/k_B T$. This allows for changes that are unfavourable with respect to energy, but of course some of these changes will be favourable with respect to the free energy because of the corresponding increase in entropy, and they can be accessed through the normal thermal fluctuations. The MC method allows for the calculation of a representative set of states in the total phase space of the system, with the correct thermodynamic weighting (i.e. higher energy states are generated less often). The procedure of proposing and testing changes in the configuration, followed by accepting or rejecting them, is repeated for many steps. If the system is started in a non-equilibrium state, the first steps will correspond to the system relaxing to an equilibrium state. Since configuration changes corresponding to large displacements of ions (e.g. swapping a pair of ions many unit cells apart) can occur, the kinetics of this process are very different to those of the real system. As a result, kinetic barriers in the real system are often eliminated in the MC method, but if the set of possible trial changes is not large, equilibrium can still be hard to reach.

The configurations generated after a reasonable period of relaxation can then be used to perform calculations of average properties. For example, the order parameter in the Ising model will have the form

$$Q = \frac{1}{N}\sum_j \pm\sigma_j$$

where the specific signs depend on the actual site in the lattice. In the MC method, it is possible to calculate the order parameter for each configuration, and then simply obtaining the grand average $\langle Q \rangle$ after many steps. Since the MC method ensures that each configuration has the correct thermodynamic weighting, the average calculated from the MC method is a good approximation to the true thermodynamic average. Similarly the average energy $\langle E \rangle$ can also be calculated. If one also calculates the corresponding mean squared values $\langle Q^2 \rangle$ and $\langle E^2 \rangle$, the susceptibility and heat capacity associated with the ordering interactions can be obtained from standard thermodynamic equations (Yeomans, 1992):

$$\chi = \beta(\langle Q^2 \rangle - \langle Q \rangle^2)$$

$$C = k_B \beta^2(\langle E^2 \rangle - \langle E \rangle^2)$$

For accurate calculations, it is necessary for the MC simulation to sample many configurations. In the MC method, as in any simulation method, the issue of statistical sampling is critical, and there will be errors associated with any calculation that reflect the quality of the statistical sampling of the complete set of configurations. For quantities that depend on the differences between averages, as in the equations for χ and C, the issue of statistical sampling is even more critical. Coupled with the issue of the need to generate many MC configurations for statistical accuracy is the issue of sample size. At an ordering phase transition, the values of both χ and C will diverge. At temperatures close to a second-order phase transition, the finite size of the sample will cause these diverges to be rounded. This problem is minimized (but never removed) by using larger samples. This will be illustrated in one of the examples discussed later in this paper.

Implementation for cation ordering

In the previous paper (Bosenick *et al.*, 2001*a*) we showed that the energy of an ensemble containing two types of atoms, which we labelled **A** and **B**, can be represented as

$$N_{\mathbf{AA}} J + E_0$$

where $N_{\mathbf{AA}}$ is the number of **A**—**A** bonds, E_0 is a constant term, and the exchange energy J is written as

$$J = E_{\mathbf{AA}} + E_{\mathbf{BB}} - 2E_{\mathbf{AB}}$$

The dependence on the number of **B**—**B** and **A**—**B** bonds is subsumed into the two terms in the energy, since the numbers of both types of bonds are completely determined by $N_{\mathbf{AA}}$. In the preceding paper (Bosenick *et al.*, 2001*a*), we outlined how this energy expression can be generalized for different cases, and how it will be expanded by taking account of different types of neighbouring atomic sites.

By itself, this energy expression is not particularly useful for MC simulations, since it is effectively an ensemble sum, and we will be interested in the ordering on individual sites in order to calculate quantities such as the order parameter. We therefore need to define a variable associated with each site that characterizes the occupancy of this site. Using the two-atom example, we can define a variable S_j associated with site j such that $S_j = 1$ if the site is occupied by an **A** atom, and $S_j = 0$ if it is occupied by a **B** atom. If we take two sites, i and j, the product $S_i S_j = 1$ if both sites are occupied by **A** atoms, and the product is zero otherwise. Thus we have

$$N_{\mathbf{AA}} = \sum_{\langle i,j \rangle} S_i S_j$$

We use the bracket notation $\langle i,j \rangle$ in the summation to denote a sum over all interactions (each counted once) rather than a double sum over all atoms (which would count each pair of atoms twice) — we will use this nomenclature throughout this paper. Similarly, the number of **A** atoms is simply given by

$$N_{\mathbf{A}} = \sum_j S_j$$

The energy can therefore be expressed in the form of the following Hamiltonian:

$$H = \sum_{\langle i,j \rangle} J_{ij} S_i S_j + \sum_i \mu_j S_j$$

where the first term is the energy associated with the bonds and the second is a chemical potential that operates if **A** atoms prefer specific sites in the crystal. The dependence of the exchange interaction J_{ij} on the specific bond reflects the fact that it will be different for different types of neighbours. For example, usually the values of J_{ij} are not found to be significantly different from zero when sites are separated by a large distance, and the largest values of J_{ij} are found for near-neighbour sites. The form of the exchange interactions for different cases is discussed in more detail in the preceding paper, together with the methods used to obtain their

values from empirical force models or quantum mechanical calculations (Bosenick *et al.*, 2001*a*).

It is common to use a 'spin variable' to define the occupancy of an atomic site for the case where there are two types of atoms. One such variable can be defined as

$$\sigma_j = 2S_j - 1$$

The spin variables σ_j have values ± 1. When we sum over interacting sites (i.e. including only bonds with a common value of J) we have terms in the Hamiltonian of the form

$$\sum_{\langle i,j \rangle} S_i S_j = \frac{zN}{4} + \frac{z}{2}\sum_j \sigma_j + \frac{1}{4}\sum_{\langle i,j \rangle} \sigma_i \sigma_j$$

The first term is clearly a constant. If there is no change in composition, the second term will also be a constant, or else it can be represented by a chemical potential. The third term is the correspondence to the bond energy. The usual chemical potential term can be added as

$$\sum_j S_j = \frac{N}{2} + \frac{1}{2}\sum_j \sigma_j$$

The main point is that there is flexibility in how the site variables (S, σ or some variation of these) and hence the Hamiltonian are expressed, although some care will always be needed to ensure that the correct factors are transferred between different representations.

When there are more than two cations, the variables used to describe the site occupancy will need to be more than simple two-valued functions. For example, if there are n cations, we can replace the site variable S by the vector $\mathbf{S}$ of length n, which will contain zero values everywhere except for the element corresponding to the label of the cation on the site. Then the Hamiltonian can be written in matrix form:

$$H = \frac{1}{2}\sum_{\langle i,j \rangle} \mathbf{S}_i^T \cdot \mathbf{J}_{ij} \cdot \mathbf{S}_j + \sum_j \mu_j^T \cdot \mathbf{S}_j$$

For example, if the sample contained Al, Mg and Fe cations, the site variables can be defined as

$$\mathbf{S}(\mathrm{Mg}) = \begin{pmatrix} 1 \\ 0 \\ 0 \end{pmatrix} \mathbf{S}(\mathrm{Al}) = \begin{pmatrix} 0 \\ 1 \\ 0 \end{pmatrix} \mathbf{S}(\mathrm{Fe}) = \begin{pmatrix} 0 \\ 0 \\ 1 \end{pmatrix}$$

It may be more convenient in this case to store the index of the non-zero element of $\mathbf{S}$ on each site rather than the whole vector (i.e. the numbers 1, 2 or 3 to represent Al, Mg or Fe in this example). $\mathbf{J}$ and μ are now of matrix form. In this example, the exchange matrix $\mathbf{J}$ would be written in diagonal form as

$$\mathbf{J} = \begin{pmatrix} J_{\mathrm{Al-Al}} & 0 & 0 \\ 0 & J_{\mathrm{Mg-Mg}} & 0 \\ 0 & 0 & J_{\mathrm{Fe-Fe}} \end{pmatrix}$$

Implementation on a parallel computer: Ossia99

Many scientific problems have parallelism in several different ways. The actual MC simulation may be parallel in its basic construction, since it involves performing similar operations on many atoms. One can imagine a strategy of splitting the ensemble across many processors and updating several sites at once. Or one could repeat the same simulation on each processor, each having a separate list of random numbers, in order to improve statistical sampling and thereby reduce the total running time. Likewise, the simulation can be run with a different temperature on each processor. Each approach represents a different type of parallelism in the problem.

We usually tend to work with the third strategy. This is partly motivated by the need to perform simulations at many state points for the calculation of the thermodynamics, as discussed below, and the exploitation of this aspect of the parallelism of the problem is easier to implement and more efficient than splitting a single simulation over many processors.

We have developed a program called Ossia99 for performing MC simulations of cation order on parallel computers. The program uses the Message Passing Interface (MPI) protocol in the programming to allow information to be passed between processors. The amount of communication that is required is kept to a bare minimum by only passing variables at the start, and then collecting all results only at the end. Writing to file is therefore left to the end. The process of reading in data, such as the range of temperatures, values of exchange interactions, and neighbour lists (discussed in more detail below), followed by assigning initial conditions for each processor, is carried out on the master processor. All relevant information is then passed to all the other processors, with each processor being assigned a subset of all the MC runs that are required. Each processor performs one equilibration run and one production run for each state point assigned to it.

During the production run various running averages are collected, and at the end of the run these are processed into a useful form. At the end of all the production runs the results are passed back to the master processor, sorted into an appropriate order, and then printed by the master processor. Each individual processor can also print out its final configuration to an assigned file. The main operation of Ossia99 is illustrated in Fig. 1.

Although written for parallel computers, Ossia99 runs equally as efficiently on a single-processor workstation. Ossia99 assumes the use of Hamiltonians of either scalar or matrix forms, and allows for the use of a chemical potential. Extension for many-site interactions is straightforward, as was needed in our simulations of Mg/Al ordering in spinel (Warren *et al.*, 2000*a,b*) discussed below as one of our main examples.

The configuration is defined in terms of a lattice of unit cells, as in a crystal. Each unit cell contains a set of labelled cation sites. The occupancies of the cation sites in each unit cell are described using the vector **S** described earlier (specifically by giving the index of the non-zero element), which allows the simulation of systems containing more than two ordering cations. The MC code is not given information about the structure of the crystal, but only about the topology of the bonds between sites. This information is provided through the use of neighbour lists, which give, for each site in each unit cell, the label and neighbouring unit cell of each interacting site. Separate neighbour lists for each site are defined for each type of exchange interaction, and are given in terms of the relative position in the lattice of the unit cell containing the neighbouring site. For example, the site #1 in each unit cell may interact with site #3 in the same unit cell and site #3 in the neighbouring unit cell along the x direction. The neighbour lists are defined in the input data file, and can be quite extensive – there is a separate neighbour list for each type of interaction. One of the merits of the spreadsheet methods discussed in the previous paper (Bosenick *et al.*, 2001*a*) is that the neighbour lists can be generated automatically. The various exchange interactions are defined using a set of matrix functions **J**.

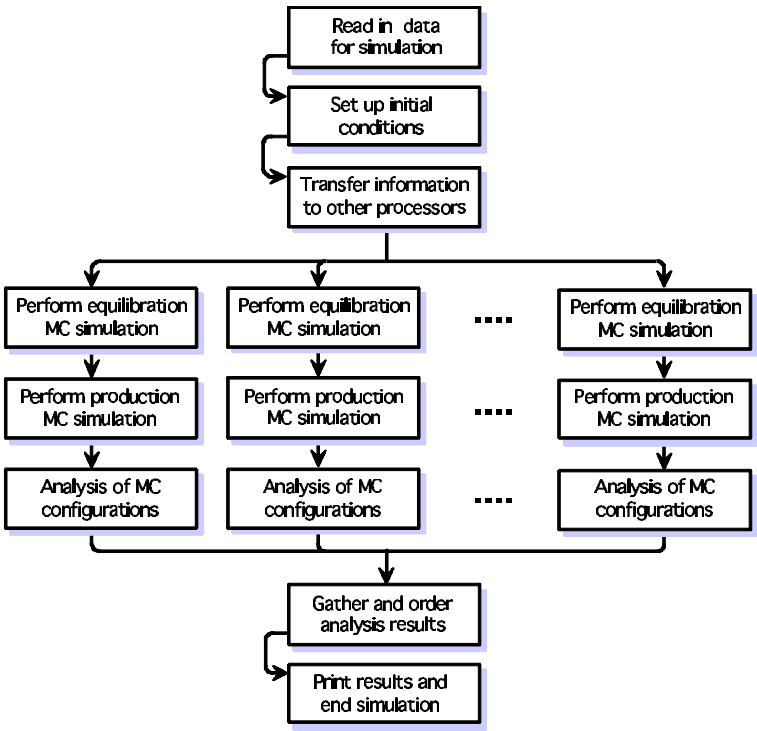

FIG. 1. Flowchart illustrating the operation of Ossia99.

An order parameter can usually be defined using the following approach. Suppose for a given site in the unit cell the occupancy with respect to one given type of cation averaged over all unit cells is s_j, such that $s_{j,0}$ is the average occupancy at $T = 0$ in the ordered structure, and $s_{j,\infty}$ is the average occupancy as $T \rightarrow \infty$. The order parameter for this site is then defined as

$$Q_j = \frac{s_j - s_{j,\infty}}{s_{j,0} - s_{j,\infty}}$$

This normalization has been chosen such that $Q = 1$ for complete long-range order, and usually the site occupancy will be unity when $Q = 1$. In complex systems, there may not be an anti-ordered state with $Q = -1$. An overall order parameter can be defined by summing over all types of cations and over all sites in the unit cell if there is only one overall ordering process, or else different order parameters that are associated with specific sites can be treated separately. Ossia99 allows the calculation of the separate order parameters for different sites, and allows $s_{j,\infty}$ to be calculated assuming a completely random mixture at high temperatures or to be given in the input file. The occupancies of the ordered structure need to be given as input, either by specifying which cations will occupy which sites, or by giving the occupancies directly. Ossia99 allows three methods to define the order parameters. In the first, the disordered occupancies $s_{j,\infty}$ are calculated as random averages of all the cations used in the simulation. In the second, the disordered occupancies $s_{j,\infty}$ are given in the input file. A third option allows the weighting of each site towards the order parameter to be set independently, to allow for very general order parameters or semi-ordered states where ordered occupancies will not all be unity. After deciding relative weightings of sites, the exact coefficients and an additive constant can be found by requiring $Q_{\text{random}} = 0$ and $Q_{\text{ordered}} = 1$. In many ordering processes the symmetry of the system may allow several ordered states to be degenerate. An example is in the ordering of cations in the mica sheets discussed below. In this case it is useful to define several order parameters and compute each of them. As one ordering process will dominate, all but one of the order parameters should have zero value, but which one may not be known in advance.

It is always possible that, with a complex Hamiltonian, the structure of the ordered phase may not be known in advance. In such a case the appropriate strategy is to plot the structure after a long run having cooled from an initial random configuration. Ossia99 allows for the final configuration on each processor to be written to a file in a form suitable for a structure-plotting program such as Cerius^{2}® or CrystalMaker®. This is also useful for analysing the structures of partially ordered or disordered structures, and will give information relevant for constructing appropriate order parameters.

The main design feature of Ossia99 is that it runs simulations at many temperatures, with different temperatures spread over the different processors. It is possible to start the simulation in an ordered (cold start) or disordered (hot start) configuration. It is also possible to start with a partial degree of order (warm start) for cases when chemical composition is not commensurate with ordering at a unit-cell level. This is implemented by defining the sites that are occupied by one set of cations, and replacing any of these at random by another set of cations subject to the final composition required. The range of temperatures can be set to have equal increments, starting from either cold or hot, or else can be run with equal increments of $1/T$, again starting from either cold or hot. The latter type of increment is particularly useful for applications with thermodynamic integration as discussed below.

Ossia99 is available from http://www.esc.cam.ac.uk/ossia, as also is an earlier version, Ossia98, which was designed specifically for the case of two types of ordering cation. The www page also provides a detailed manual.

Examples of long-range ordering behaviour

Simple Al/Si ordering in a three-dimensional structure

In Fig. 2, we show the calculation of the order parameter Q and inverse susceptibility χ^{-1} calculated for an equal mixture of two types of cation on an ideal tridymite lattice (Dove, 1999; Dove *et al.*, 2000). The results are typical of the ordering behaviour of a simple system, with a continuous change in Q on approaching the transition temperature from below. The results are not equivalent to those given by a simple mean-field type theory, such as Bragg–Williams, where one would expect the following two relationships (Yeomans, 1992):

$$Q_{\text{mft}} \propto (T_c - T)^{1/2}; \chi_{\text{mft}} \propto |T_c - T|^{-1}$$

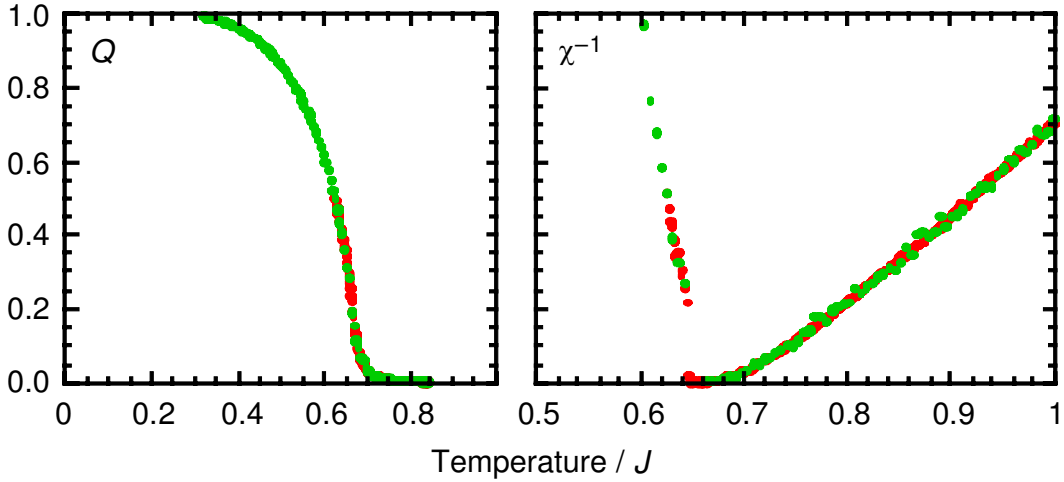

FIG. 2. Temperature dependence of the order parameter Q and inverse susceptibility χ^{-1} for a system containing equal numbers of Al and Si cations on a kalsilite ($KAlSiO_4$) network of tetrahedral sites, obtained from MC simulations. Different coloured points represent different simulation runs.

These mean-field relationships are not found in any of the examples of ordering phase transitions we will show in this paper. Instead, Q tends to fall more rapidly on heating towards T_c. Most of the models we investigate fall into classes for which the following variations are found (Yeomans, 1992)

$$Q(T \rightarrow T_c) \propto (T_c - T)^{\beta}; \chi(T \rightarrow T_c) \propto |T_c - T|^{-\gamma}$$

with $\beta < 1/2$ (typically closer to 1/3 for three-dimensional systems, or 1/8 for two-dimensional systems), and $\gamma > 1$ (typically closer to 4/3 for three-dimensional systems).

The results shown in Fig. 2 highlight the point (made earlier) about finite sample sizes causing a rounding of the phase transition. This can be seen as the tail in the order parameter above the phase transition, instead of the order parameter falling sharply to zero. Rounding effects can also be seen in the plot of χ^{-1}.

Ordering in two-dimensional hexagonal nets representative of cation ordering in mica sheets

In Fig. 3 we show a hexagonal net representing the layers of tetrahedral or octahedral sites in a mica. Models of the ordering interactions (Bosenick *et al.*, 2001*a*; Palin *et al.*, 2001) have shown that the four exchange interactions defined in Fig. 3 are positive for both Al/Si and Mg/Al ordering, with J_1 having the largest value and J_3 the smallest. Thus ordering is driven by the need to minimize the number of neighbours containing the same types of cations. For a 1:3 ratio of two types of cations, whether Al:Si on the tetrahedral sites or Mg:Al on the octahedral sites, the ordered structure within a layer is found to be that shown in Fig. 3. This is distinguished from other possible ordering processes by the sign of J_4 (Palin *et al.*, 2001). The MC simulations were performed by Al/Si ordering in the tetrahedral sites of muscovite, $K_2Al_4(Si_6Al_2O_{20})(OH)_4$ (Palin *et al.*, 2001). The ordering phase transition is very sharp, as indicated by the temperature dependence of the order parameter, heat capacity and susceptibility shown in Fig. 4. In this figure we compare the ordering within isolated layers with the ordering when we included three-dimensional interactions between the tetrahedral sheets. The main details are very similar in both cases, except that in the three-dimensional simulation the transition has been shifted to a slightly higher temperature and the phase transition is even sharper. Detailed analysis of the results for the order parameter show that on heating up to T_c the order parameter follows the analytical form of the two-dimensional Ising-model order parameter (Yeomans, 1992):

$$Q(T \rightarrow T_c) \propto (T_c - T)^{1/8}$$

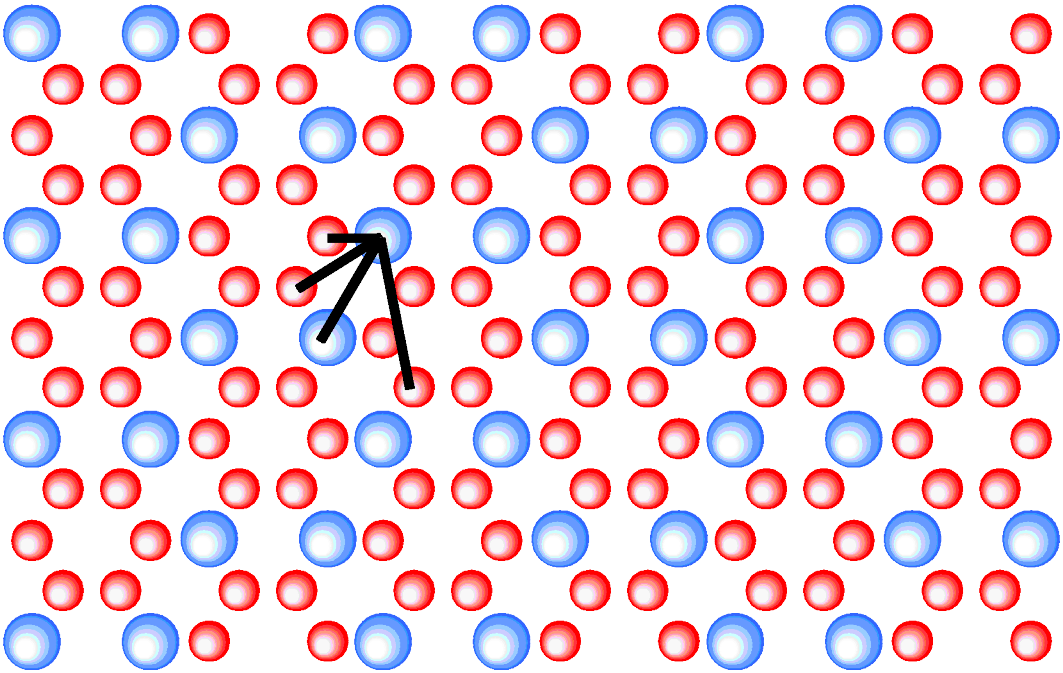

FIG. 3. Hexagonal net representing the two-dimensional layers of tetrahedral or octahedral sites in the mica structure. The two sizes/colours of spheres show the ordered patterns for a 1:3 ratio of two types of cations as given by the exchange interactions for Al/Si (Palin *et al.*, 2001) or Mg/Al ordering (from Bosenick *et al.*, 2001*a*) as calculated using the methods of Bosenick *et al.* (2001*a*). The four lines indicate the neighbours for which exchange interactions were defined.

The phase transition in the three-dimensional simulation could only be studied starting from a fully ordered structure and heating from cold. It appeared that if the simulation started from a completely random arrangement of cations, the individual layers would order independently on cooling, and it was not possible for the ordered arrangements in each layer to then shift to be in register with their neighbouring layers. Whilst this highlights one of the intrinsic problems of the MC method, namely that of having only a finite simulation time, it does show that the kinetic problem may be also be faced in establishing long-range order in natural samples.

Using a warm start (as defined earlier), it was possible to study how the ordering process within a layer will change when the composition changes from 1:3 towards 1:7 as found in some micas. The results are shown in Fig. 5. Although a clear phase transition is observed with composition of 1:3, no ordered state was found for a single layer with 1:7 composition. In this case, the interactions do not have sufficient range to form a continuous network between sparse Al cations. As the concentration of Al decreases from 25%, this loss of any long-range ordering process can be seen in Fig. 5.

Coupled Al/Si and Mg/Al ordering in mica structures

We have explored coupled ordering in the mica phengite, $K_2(Al_3Mg)(Si_7Al)O_{20}(OH)_4$. This is similar to muscovite, except that there is a coupled-charge substitution of replacing an Al by Mg in the octahedral layer and the replacement of an Al by Si in the tetrahedral layers. Now we have two ordering processes, Al/Si in the tetrahedral layers, and Mg/Al in the octahedral layers, with a coupling between the two layers. The development of an appropriate model Hamiltonian is sketched briefly in the previous paper (Bosenick *et al.*, 2001*a*). The exchange interactions within both the tetrahedral and octahedral layers favour the ordered patterns shown in Fig. 3 for both types of layers. However, we now have only half the number of

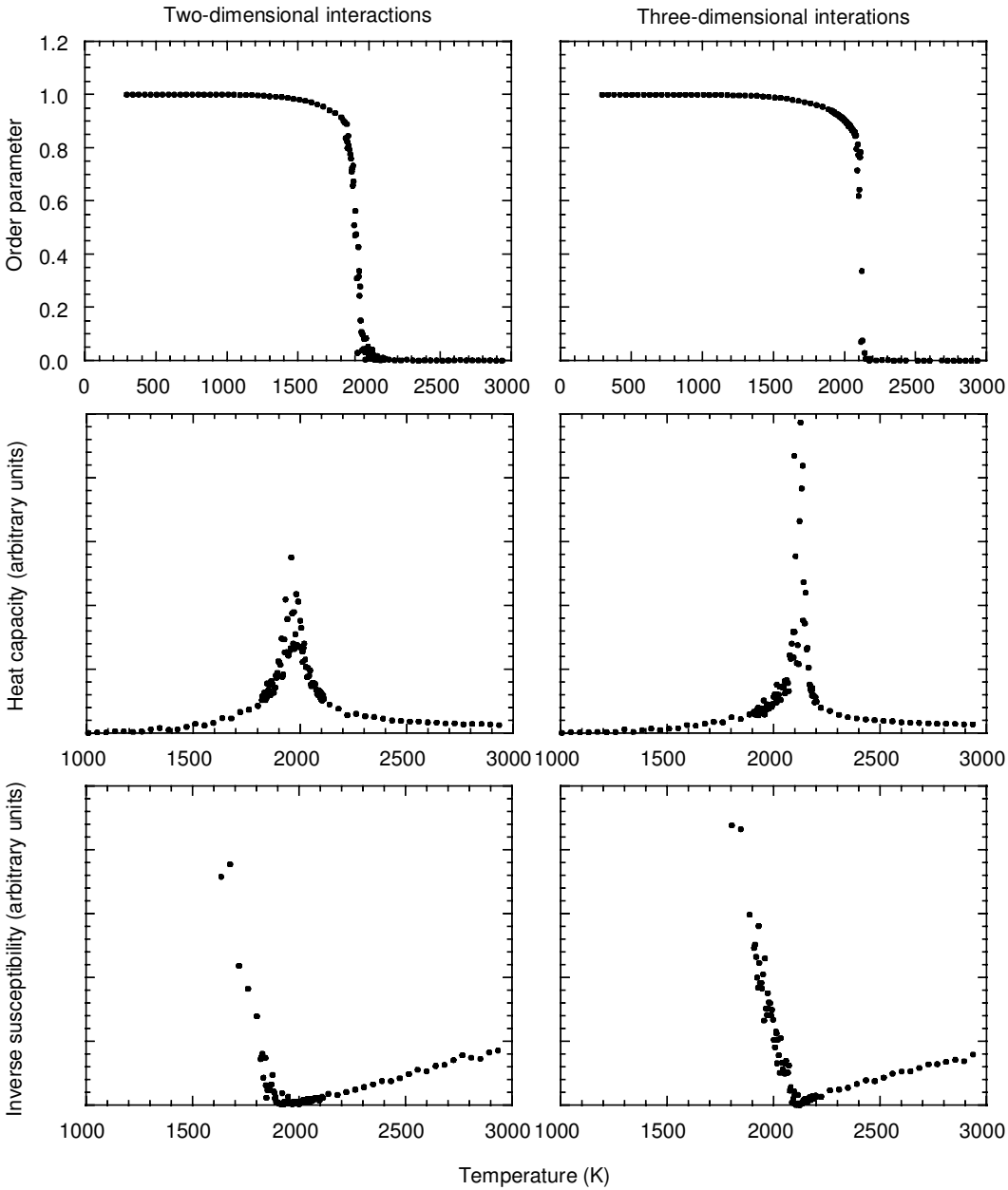

FIG. 4. Temperature dependence of the order parameter, heat capacity and inverse susceptibility, χ^{-1}, for Al/Si ordering in the tetrahedral sheets in muscovite, $K_2Al_4(Si_6Al_2O_{20})(OH)_4$, obtained from MC simulations performed with and without three-dimensional interactions between neighbouring layers of tetrahedra (Palin *et al.*, 2001). The behaviour close to the transition temperature is like that of a two-dimensional Ising model.

Al cations in the tetrahedral sheets, and it was shown in Fig. 5 that the tetrahedral sheets on their own will not order with such a low Al:Si ratio. However, ordering is possible when there are

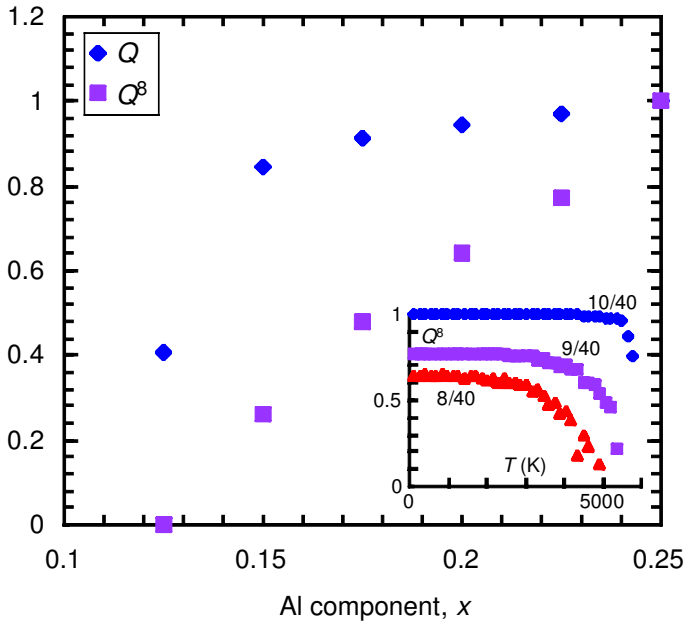

FIG. 5. Variation of the order parameter Q for the two-dimensional Al/Si ordering phase transition in tetrahedral layers of muscovite with chemical composition Al_xSi_{1-x}. The main figure shows the dependence of Q and Q^8 on Al composition x at low temperatures. The inset in the lower right corner shows the temperature dependence of Q^8 for three compositions. The phase transitions are very sharp, and variations are better seen through plots of Q^8 than Q, following the comment in the text that in two dimensions the temperature dependence of Q is $Q \propto (T_c - T)^{1/8}$.

interactions mediated through other layers. In the case of phengite, the MC simulations using the model Hamiltonian give a more complex ordered structure, as shown in Fig. 6. This shows an octahedral layer with one of its neighbouring tetrahedral layers. The exchange interactions favour the formation of Al—Al pairs on neighbouring octahedral and tetrahedral sheets, and this can best be achieved by having the octahedral sites order in a way that is less favourable for the interactions within the octahedral layers. Specifically, the favoured layer ordering has only third-neighbour Mg—Mg pairs, but the coupling with the tetrahedral layers forces the ordering to have only second-neighbour Mg—Mg pairs. The ordering in the tetrahedral layers is based on that obtained in muscovite, but with half of the Al replaced by Si. This arrangement ensures that there are no $Mg^{[6]}$—$Al^{[4]}$ neighbours, as seen in Fig. 6.

The MC simulations also showed an interesting ordering sequence. On cooling (heating), the ordering (disordering) in the tetrahedral layers does not lock in as a single process, but as a two-stage process. The first process on cooling involves half the tetrahedral sites becoming occupied by Si, and the other half being disordered with 75% occupancy by Si and 25% occupancy by Al. These sites are indicated in Fig. 6. This first process is coupled with the ordering on the octahedral sites. The second set of tetrahedral sites only order at a temperature about half of that of the first ordering process. The details of this ordering sequence are still being investigated, but are described here to illustrate the point that relatively complicated behaviour can arise when a system contains competing ordering processes.

Non-convergent ordering in spinel, $MgAl_2O_4$

The ordering process in spinel involves exchange of Mg and Al cations between octahedral and tetrahedral sites. This process does not involve a change in symmetry and therefore does not precipitate a phase transition, but there are many

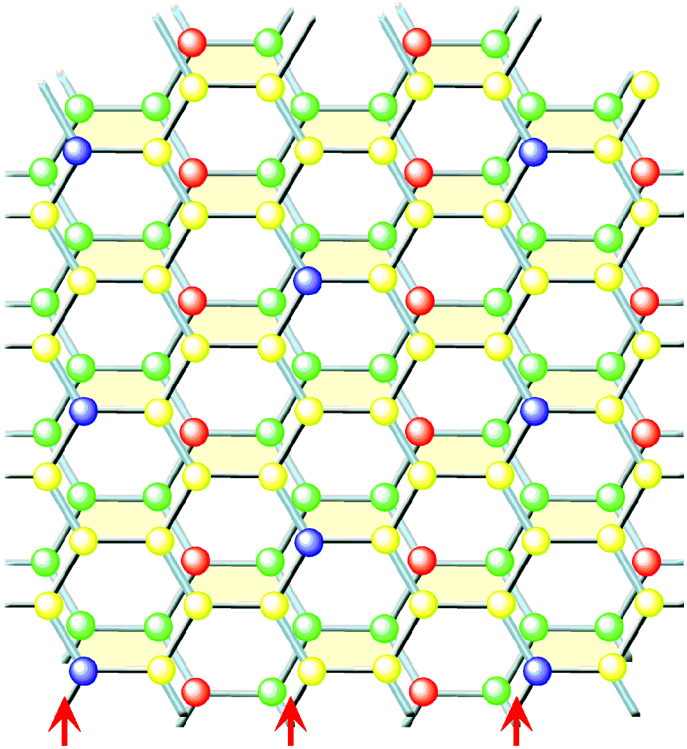

FIG. 6. The ordered structure of phengite, $K_2(Al_3Mg)(Si_7Al)O_{20}(OH)_4$, as predicted by the MC simulation using the model Hamiltonian developed by Bosenick *et al.* (2001*a*). The structure shows the octahedral layer of Mg/Al cations and one neighbouring tetrahedral layer of Al/Si cations. The cations in both layers are arranged on a hexagonal grid, with the two grids displaced with respect to each other. The second tetrahedral layer attached to the octahedral layer is displaced in the opposite direction. The tetrahedral layer is drawn above the octahedral layer. The Al and Si cations in the tetrahedral layer are coloured blue and yellow respectively, and the Mg and Al cations in the octahedral layer are coloured red and green respectively. The red vertical arrows indicate the chains of tetrahedral sites that remain disordered with respect to the positions of the Al and Si cations on first cooling below the temperature at which the octahedral layer begins to order.

aspects of the ordering process that resemble the behaviour associated with a phase transition. This type of ordering process is called non-convergent ordering, and although there is a not a distinct phase transition, many systems displaying non-convergent ordering processes have a temperature dependence that can be described using methods commonly applied to the study of phase transitions (Carpenter *et al.*, 1994; Carpenter and Salje, 1994).

An order parameter can be defined that is determined by the occupancy of the cations on the two types of sites. The MC simulations were performed using a model Hamiltonian that was parameterized using *ab initio* quantum mechanics methods (Warren *et al.*, 2000*a*,*b*; Bosenick *et al.*, 2001*a*). The calculated temperature-dependence of the order parameter is shown in Fig. 7, where it is compared with experimental measurements obtained by neutron diffraction data (Redfern *et al.*, 1999). The experimental data at low temperatures are not able to reach equilibrium values because of kinetic constraints, and the comparison with the simulation data is not relevant. At temperatures above 900 K, where the experimental data do correspond to equilibrium, the agreement of the MC results with the experimental data is very good. The remarkable point about the level of agreement is that it was achieved without the use of any experimental data

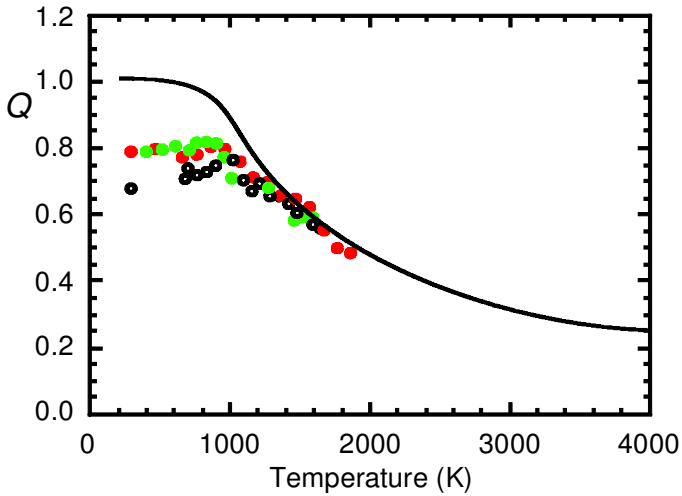

FIG. 7. Temperature dependence of the order parameter for Mg/Al non-convergent ordering in spinel calculated by MC simulations (Warren *et al.*, 2000*a,b*) and compared with experimental neutron diffraction data (Redfern *et al.*, 1999). The experimental data for temperatures below 900 K are lower than equilibrium values because of kinetic limitations. Three different experimental runs are coloured differently. The ordering in these runs follows different kinetic histories, leading to different degrees of order at low temperatures.

in the development of the model Hamiltonian. The good agreement provides some validation of the use of the model Hamiltonian, as discussed in Bosenick *et al.* (2001*a*).

Cation ordering in the pyroxene diopside—Ca-Tschermak solid solution

In the solid solution diopside–Ca-Tschermak, $Ca[Mg_xAl_{1-x}]^{VI}[Si_{1+x}Al_{1-x}]^{IV}O_6$ with $0 \leqslant x \leqslant 1$, the substitution of Al^{3+} for Si^{4+} on the tetrahedral sites is coupled with the substitution of Al^{3+} for Mg^{2+} on the M1 octahedral sites. In the end-member Ca-Tschermak, where $x = 0$, half of the tetrahedral sites are occupied by Si and half by Al cations. For this pyroxene, there are four possible long-range ordered structures with complete ordering of Al and Si on the tetrahedral chains consistent with the Al—Al avoidance for nearest neighbour tetrahedral sites along the chains. Their corresponding space groups are $C2$, $C\bar{1}$, $P2/n$ and $P2_1/n$ (Okumara *et al.*, 1974). Experimentally, only the disordered high-temperature structure ($C2/c$) has been observed. Static lattice energy calculations predict the $P2_1/n$ structure to be the most favourable ordering state energetically. The MC simulations of the ordering process in Ca-Tschermak based on a model Hamiltonian constructed from empirical potential calculations, as described in the previous paper (Bosenick *et al.*, 2001*a*), place the transition from $C2/c$ to $P2_1/n$ at a temperature of ~1500 K. As will be described below, NMR data indicate that this value is an overestimate (Bosenick *et al.*, 1999*a*), and a one-point temperature calibration would place the transition temperature just below 1000 K. However, at temperatures below ~1400 K, Ca-Tschermak is thermodynamically unstable with respect to conversion to grossular and corundum (Gasparik, 1984). This explains why no ordered Ca-Tschermak has been found experimentally. On the other hand, the effects of the ordering interactions will be seen in the short-range order at temperatures substantially above T_c, well into the stability range of Ca-Tschermak.

In the solid solution, $x > 0$, there is also ordering of Al and Mg on the octahedral sites, in addition to ordering of Al and Si on the tetrahedral sites. These two ordering processes are not independent because there are interactions between the cations in the tetrahedral and octahedral sites. Because of this complex ordering behaviour, it is not straightforward to derive possible ordering patterns for the solid-solution composition by theoretical considerations as could be done for Ca-Tschermak. The lowest-

energy state, based on a set of exchange interactions determined by lattice energy calculations (Bosenick *et al.*, 2001*a*), can be determined for any composition by MC simulations. In the case of $x = 0.5$, Di50:CaTs50, the lowest energy configuration given by the MC simulations had a repeating —Al—Si—Si—Si— arrangement along the tetrahedral chains, a repeating —Mg—Al—Mg—Al— arrangement along the octahedral chain, and relative arrangements on the chains of tetrahedra and octahedra that form Al—Al linkages in neighbouring tetrahedral and octahedral sites. In comparison to the high-temperature disordered structure with space group $C2/c$, the ordered structure has a unit-cell that has been doubled in the c direction, with space group $C2$. This structure is shown in Fig. 8. The MC simulations of the ordering process show that the transition temperature for this ordering process is substantially below that of the Al/Si ordering in the CaTs end-member.

Short-range order

Short-range order in the MC simulations and NMR data

The energy computed in a MC simulation arises directly from the short-range interactions, which means that information about the short-range structure is readily available from the simulations. There may be many ways of defining the short-range structure, but the most useful procedure for many cases is to compute the components of the short-range structure that are detected in an experiment.

The most direct experimental technique for the measurement of short-range order is magic-angle spinning (MAS) NMR (Putnis and Vinograd, 1999). In principle, the spectra from this technique for appropriate isotopic species will give a single peak for each cation of the species in each different environment. There are two factors that determine the frequency of each peak in the MAS-NMR spectra. The first is that the specific type of site can have a significant effect. For example, the crystal structure of cordierite, $Mg_2Al_4Si_5O_{18}$, has two distinct types of tetrahedral site, one of which is in a six-membered ring of tetrahedra, and the other in a four-membered ring. The frequencies of the peaks in the spectra can be correlated with the type of site if the types of site are sufficiently different. In cordierite the two types of site can clearly be distinguished in the MAS-NMR data (Putnis *et al.*, 1985). However, the intrinsic resolution of the MAS-NMR spectra means that atoms in very similar sites are hard to distinguish. So if there is a structural phase transition, whether displacive or cation order/disorder, that causes two sites that are equivalent in one phase to become inequivalent in the other, it is quite possible that the splitting of the peak will not be easily resolved. The second factor is that there are shifts in the positions of peaks due to differences in the local environments of sites that are equivalent on average. For example, in cordierite it is possible to distinguish separate peaks in the spectrum associated with Si having different numbers of Al cations (from 0 to 4) in the neighbouring tetrahedral sites (Putnis *et al.*, 1985). For the pyrope–grossular garnet solid solution it was possible to resolve the effects on the Si-MAS-NMR spectra of changing the number of Mg/Ca cations in both the first and second co-ordination shells (Bosenick *et al.*, 1995, 1999*b*). These different environments correspond to different types of small clusters of cations. In principle, the intensities of the peaks associated with each type of environment in any system will directly give the relative proportions of the different types of clusters. From an analysis of the statistics of bonds (as discussed in the previous paper, Bosenick *et al.*, 2001*a*) it is also possible, at least in principle, to use the MAS-NMR data to determine the numbers of other types of bonds, such as the numbers of Al—Al linkages.

The relative proportions of the clusters of cations corresponding to those detected in an MAS-NMR experiment are easy to calculate in a MC simulation with Ossia99 (although the definitions need to be given by the user at the start of the simulation, and some manipulation of the code will be necessary). The calculation of the MAS-NMR cluster proportions is useful in three respects. First, it enables comparison to be made between MAS-NMR results and the thermodynamic state of the material, which can be calculated in the MC simulation using methods outlined later. Second, the comparison of the MC results with MAS-NMR data enables the simulation to be better calibrated. For example, it may be shown whether the temperature scale in the simulations, which is set by the energy scale of the model Hamiltonian, is accurate. Third, assuming that the energy scale of the model is accurate, the correlation of MC results and experimental MAS-NMR data for materials that are prepared under non-equilibrium conditions may provide information about the state of

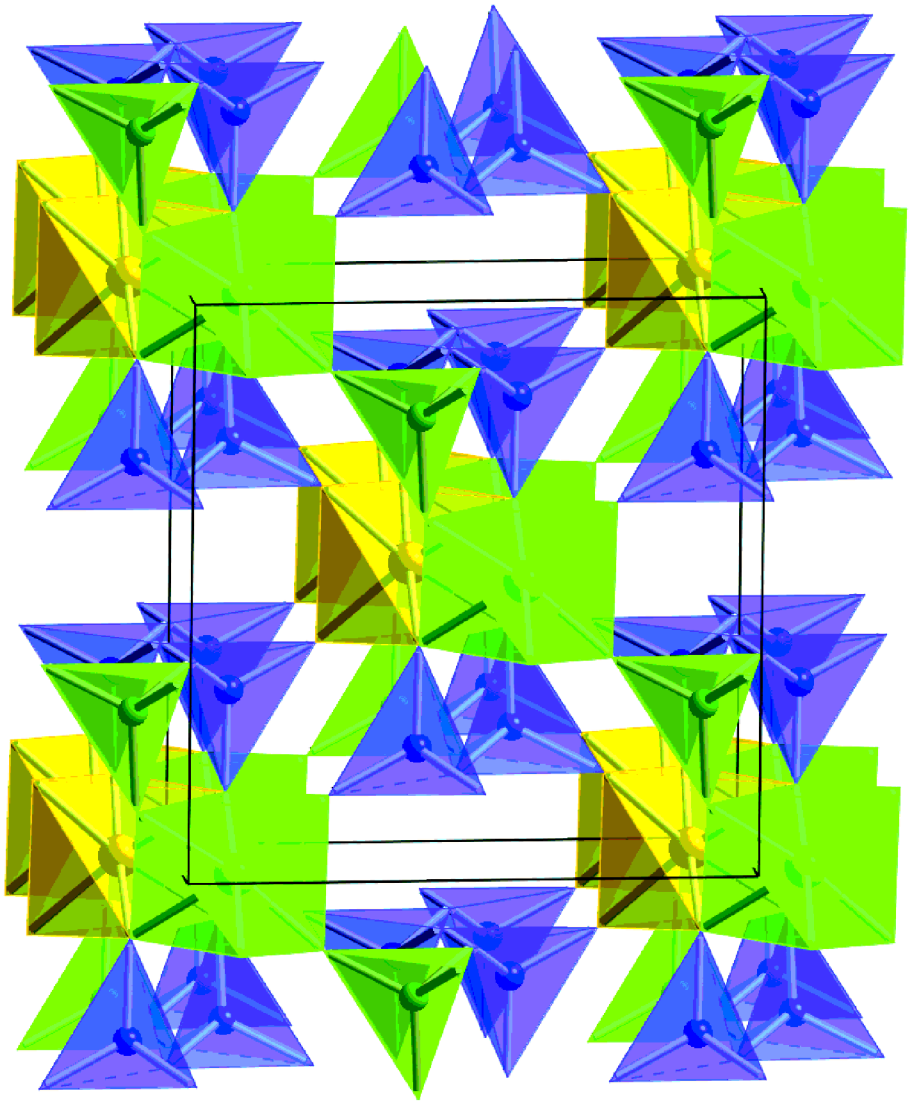

FIG. 8. Predicted ordered structure of the 50:50 diopside–Ca-Tschermak structure. The SiO_4 tetrahedra are coloured blue, the MgO_6 octahedra are coloured yellow, and the AlO_4 tetrahedra and AlO_6 octahedra are coloured green. The Ca cations are not drawn in order to assist clarity. The ordered structure was obtained by MC simulation cooling to low temperature, using a model Hamiltonian with exchange interactions described in Bosenick *et al.* (2001*a*).

ordering and the balance between long-range and short-range order in the material.

The discussion here has assumed that the MAS-NMR data can be interpreted unambiguously. However, it is often the case that peaks in the MAS-NMR spectra overlap so that it is not possible to obtain the intensities of all individual peaks separately. This was found for some of the garnet compositions studied by Bosenick *et al.* (1995). However, a good MC simulation will facilitate interpretation of MAS-NMR data. This is one of the applications that will characterize our examples given below.

It is important to remark regarding the comparison between experimental MAS-NMR data and the results of the MC simulations that

one might expect that even a poor model could give a reasonable level of agreement with experimental data. This is because only a small fraction of all possible configurations are encompassed in the subset between fully ordered and fully disordered, and if the MC Hamiltonian gives the correct ordered structure it may be that the main features of the MAS-NMR data (particularly whether peaks are strong or weak) will be relatively easy to reproduce.

Short-range order in the garnet pyrope–grossular solid solution

In Fig. 9 we show the temperature dependence of the intensities of the stronger MAS-NMR peaks in the garnet pyrope–grossular solid solution, $(Mg_xCa_{1-x})_3Si_3Al_2O_{12}$, calculated in the MC simulations and measured experimentally (Bosenick *et al.*, 1995, 1999*b*). In this case the MAS-NMR technique is sensitive to the presence of both first and second-neighbour shells of atoms about the Si cations. The first shell contains 2 Mg/Ca cations, and the second shell contains 4 Mg/Ca cations. The first shell can be occupied in three different ways: (2Mg0Ca, 1Mg1Ca or 0Mg2Ca), while there are five ways to occupy the second shell (4Mg0Ca, 3Mg1Ca, 2Mg2Ca, 1Mg3Ca or 0Mg4Ca). The combination of different first and second shell configurations results in $3 \times 5 = 15$ different possible Mg/Ca clusters. In Fig. 9 the clusters have been labelled according to the dominant cation in the first and second shell. For example, for Mg-rich composition, in the cluster (2,4) the first and second shell are only occupied by Mg-cations, and in the cluster (1,0) the first shell contains 1 Mg and 1 Ca cation while the second shell has 4 Ca cations.

In principle, each of the 15 clusters should correspond to an individual ^{29}Si MAS-NMR resonance. However, in practice some of the clusters have very similar chemical shifts, and therefore their peaks overlap in the MAS-NMR spectra. Therefore, not all of the observed MAS-NMR resonances can be assigned unequivocally to specific clusters. In addition, depending on the garnet composition, some of the clusters have a low occupancy and their MAS-NMR peaks were not observed experimentally. This may have led to systematic errors in the determination of the relative MAS-NMR resonance intensities which will affect the comparison with the simulation data. Another reason why the correspondence between MAS-NMR intensities calculated in the MC simulations and the experimental data is not as good as possible could be related to inadequacies in the simulation methods. For example, the model used in the simulation is symmetric for compositions either side of the midpoint of the solid solution (Bosenick *et al.*, 1999*a*, 2000, 2001*a,b*), and this symmetry may not be present in the experimental data (see discussion in Bosenick *et al.*, 2001*b*).

Aside from the details of the comparison between the experimental data and the MC simulation, one important aspect of the comparison between the calculated and observed MAS-NMR cluster probabilities is the extent to which they depart from their random values, and how the probabilities change as a function of temperature. In this regard, the simulations have mixed success — in particular, they are better for the dilute mixtures than for compositions nearer 50%. In the case of Mix 85:15, the simulations reflect the experimental data on Py85:Gr15 in that there is little departure from the random values and very little variation with temperature. For Mix 75:25 the trends in the resonance intensities observed in the MAS-NMR spectra of Py75:Gr25 synthesized at different temperatures are in agreement with those predicted with the MC simulations. The proportions of clusters (2,4) and (1,4) increase, while those of clusters (2,3) and (1,3) decrease simultaneously. However, in the experiment, the proportion of cluster (2,4) becomes larger than that of cluster (2,3) for the lowest synthesis temperature. This crossover is not predicted in the simulation.

Short-range order in muscovite

Our second example of the calculation of short-range order is for Al/Si ordering in muscovite. Figure 10 shows the calculated temperature dependence of the Si MAS-NMR spectra, in which different peaks correspond to different numbers of Al neighbours. The MAS-NMR spectra change on cooling as the short-range order within the tetrahedral layers drives the formation of long-range order. One striking point is that the calculated intensities only approach the values for completely random order at extremely high temperatures (well above the melting and vapour temperatures!).

There have been several MAS-NMR studies of muscovite at ambient temperature, with attempts to interpret the data in terms of different models of order and ordering mechanisms (Herrero *et al.*,

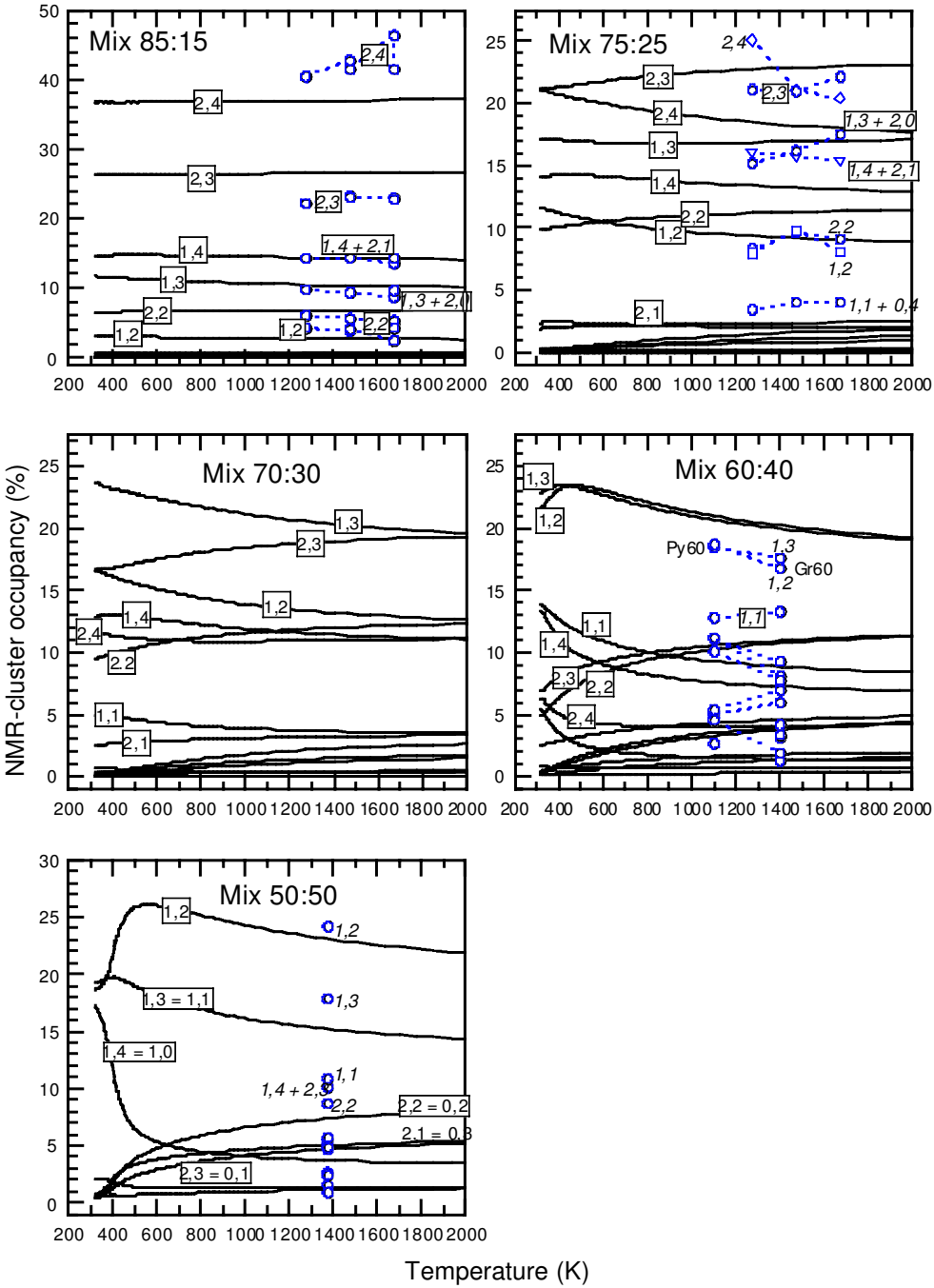

FIG. 9. Temperature dependence of the ^{29}Si MAS-NMR peak intensities in the pyrope–grossular solid solution calculated by MC simulations (Bosenick *et al.*, 2000) and compared with experimental data (Bosenick *et al.*, 1995, 1999*b*). The labels on the lines represent the occupancies of the two shells of Mg/Ca sites around the Si tetrahedral site, and are defined in the text.

1985, 1986, 1987, 1989; Herrero and Sanz, 1991; Circone *et al.*, 1991). The experimental data were obtained for different compositions, and values extrapolated for the simulation samples are given in Fig. 10. For both sets of data (Herrero *et al.*, 1987; Circone *et al.*, 1991) the intensities of the peaks in the MAS-NMR spectra, when compared to the MC results, correspond to temperatures just above the temperature at which long-range order is established. At this temperature there is a reasonable amount of short-range order. This implies that muscovite is formed with a high-

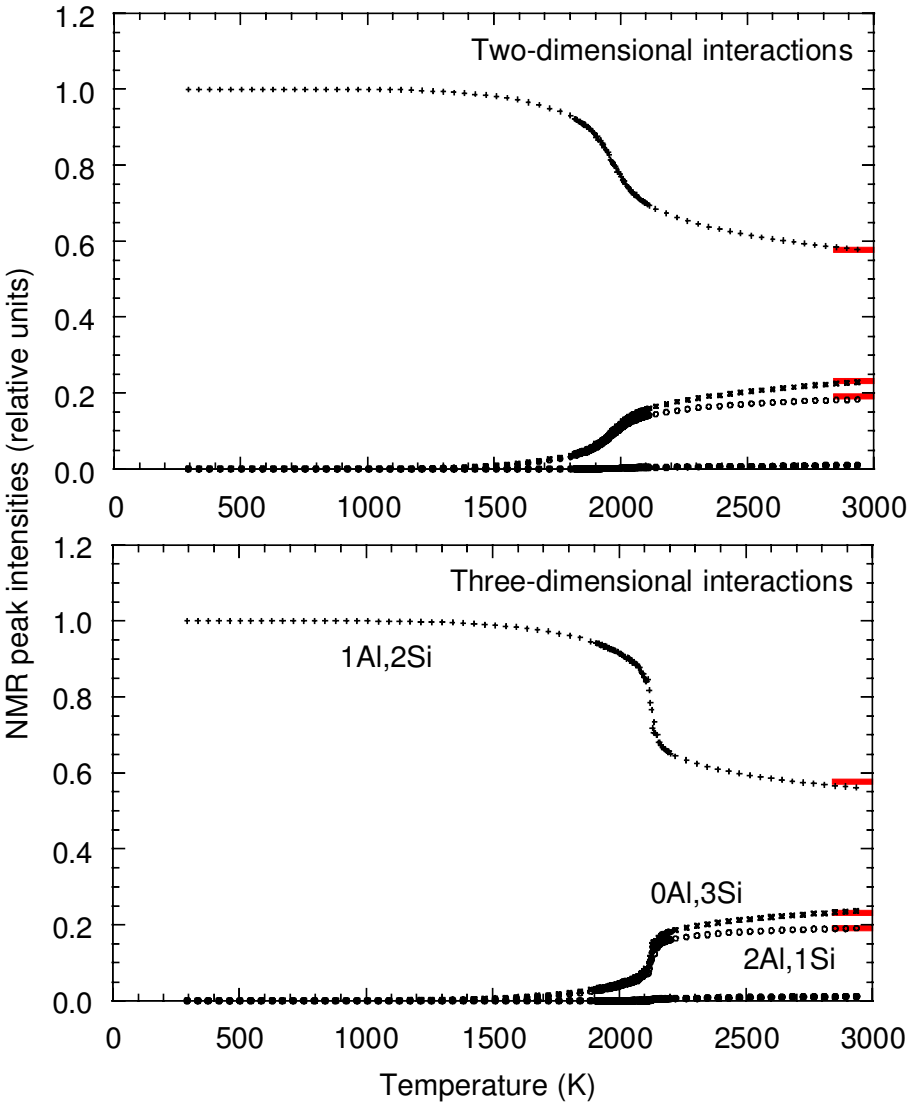

FIG. 10. Temperature dependence of the ^{29}Si MAS-NMR peak intensities in muscovite calculated by MC simulations using both two-dimensional and three-dimensional models (Palin *et al.*, 2001). The red horizontal lines on the right hand side of each plot represent the experimental values interpolated from the data of Herrero *et al.* (1987), as discussed by Palin *et al.* (2000). The important point is that the experimental data are consistent with no long-range order but considerable short-range order, corresponding to an equilibrium temperature just above the transition temperature for long-range order.

temperature distribution of cations that is then frozen into the structure as a non-equilibrium state of order. The point of interest here is that the MC simulations were able to give a clear interpretation of the MAS-NMR results that was not possible otherwise.

Short-range order in the diopside–Ca-Tschermak solid solution

^{29}Si MAS-NMR spectroscopy data for several compositions in the diopside–Ca-Tschermak solid solution series are shown in Fig. 11 (our own data reported by Bosenick *et al.*, 1999*a*, which are in accord with the data of Millard and Luth, 1998). In the end-member Ca-Tschermak, ^{29}Si MAS-NMR spectroscopy gives the Al/Si distribution around the ^{29}Si nuclei in the tetrahedral chains. Figure 12*a* shows the temperature dependence of the three MAS-NMR clusters (2Si0Al, 1Si1Al, 0Si2Al) from MC simulations. The relative peak intensities observed for a synthetic Ca-Tschermak synthesized at 1748 K match the MC occupancies at a temperature of ~2700 K. When this data point is used to perform a one-point temperature calibration of the MC temperature scale, the transition temperature for the ordering phase transition is shifted from ~ 1500 K to below 1000 K (as discussed above in the section on long-range order).

The ^{29}Si MAS-NMR spectra of members of the diopside-Ca-Tschermak solid-solution shown in Fig. 11 have four broad resonances (Millard and Luth, 1998; Bosenick *et al.*, 1999*a*). Hence, in addition to the Al/Si distribution on the two neighbouring corner-sharing tetrahedra, the ^{29}Si MAS-NMR spectroscopy must also be sensitive to different second-shell neighbours in the solid-solutions. These second neighbours correspond to three neighbouring M1 octahedra that are corner-shared with the tetrahedron that contains a ^{29}Si nucleus. In the solid-solution, they can be occupied in four different ways: 3Mg0Al, 2Mg1Al, 1Mg2Al or 0Mg3Al. We ignore the fact that these three M1 octahedra are not symmetrically arranged around the tetrahedron. A combination of all possible first and second shell configurations results in $3 \times 4 = 12$ different clusters. The clusters will be labelled according to the number of Al neighbours on tetrahedral and octahedral sites, i.e. (nAl^{IV},nAl^{VI}).

The assignment of the resonance peaks in the MAS-NMR spectra to the different clusters is complicated by the fact that the substitution of Al for Si in the neighbouring tetrahedral sites results in a positive change in the chemical shift, whereas the substitution of Al for Mg on the corner-sharing octahedra results in a negative change in the chemical shift. The absolute changes in the chemical shifts should be larger for a substitution in the 1st shell compared to a substitution on the 2nd shell, because of the smaller distance to the MAS-NMR active nuclei. However, as only four broad resonances are observed, in comparison to the twelve possible clusters, it is clear that several clusters must have similar chemical shifts and that peak overlapping is present in the spectra. This problem is not uncommon in the use of MAS-NMR methods to study cation order, and the following discussion will show how MC simulations can be used to help interpret the MAS-NMR spectra.

The temperature dependence of the relative occupancy of the 12 clusters in Di50CaTs50 determined with MC simulations is plotted in Fig. 12*b*. Above the transition temperature, there are no dramatic changes in the cluster occupancy. In the lower part of Fig, 12*b*, we compare the experimental MAS-NMR peak intensities, with two different MAS-NMR peak assignments, i.e. the occupancies of those clusters that are believed to overlap in the MAS-NMR spectra are summed together.

The MAS-NMR peak assignment used in the lower left part of Fig. 12*b* is based on the proposal that the chemical shifts of clusters having 1, 2 and 3 octahedral Al are very similar, and hence that the ^{29}Si MAS-NMR is only sensitive to whether Al is present in the second shell (n, Al) or not (n, 0) (Millard and Luth, 1998; Putnis and Vinograd, 1999). The agreement between this interpretation of the observed MAS-NMR intensities and the MAS-NMR cluster occupancies from the MC simulations is very poor. For example, the relative intensity of the MAS-NMR peak at −80.6 ppm is 33% but the combination of the occupancies of clusters (1,0) and (2,Al), where cluster (2,Al) is the sum of clusters (2,1), (2,2) and (2,3), gives a maximum relative intensity of 11%. These discrepancies are unlikely to be due to inadequacies in the MC simulations, but instead they probably indicate that the peak assignment is not correct. Based on the cluster occupancies from the MC simulations, a modified peak assignment has been obtained, and is given in the lower right part of Fig. 12*b*. This new assignment results in a much better agreement with the observed MAS-NMR peak intensities, and also gives a much

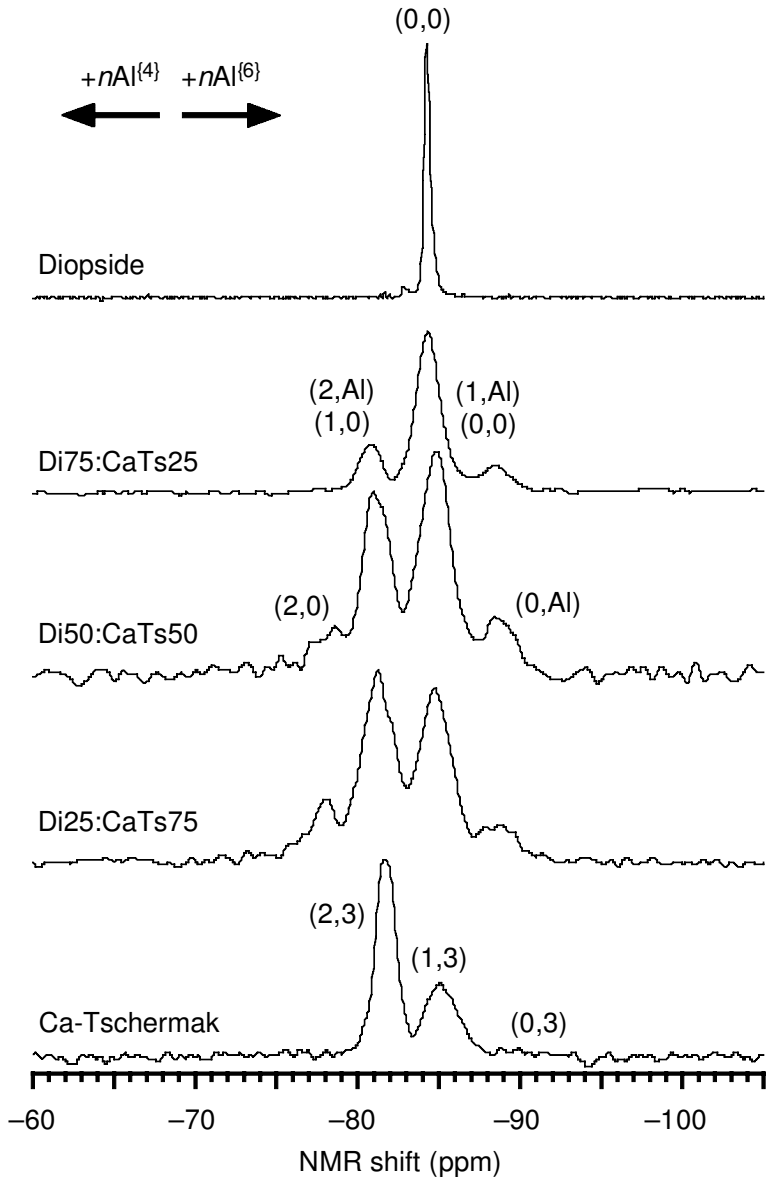

FIG. 11. ^{29}Si MAS-NMR spectra of members of the diopside–Ca-Tschermak solid solution for several different compositions, previously reported by Bosenick *et al.* (1999*b*) and consistent with the data of Millard and Luth (1998). The labels represent the interpretation of Putnis and Vinograd (1999); the definitions are given in the text. The arrows at the top show the directions of the shifts of the peaks due to increases in the number of Al cations in the neighbouring octahedral and tetrahedral sites (Putnis and Vinograd, 1999).

better agreement with the experimental MAS-NMR data for compositions Di75CaTs25 and Di25CaTs75. The MAS-NMR data have thus been interpreted using the MC results to give an assignment that might not otherwise have been found. This is an example of how the MC simulation method is able to help to derive a reliable MAS-NMR peak assignment, which

a

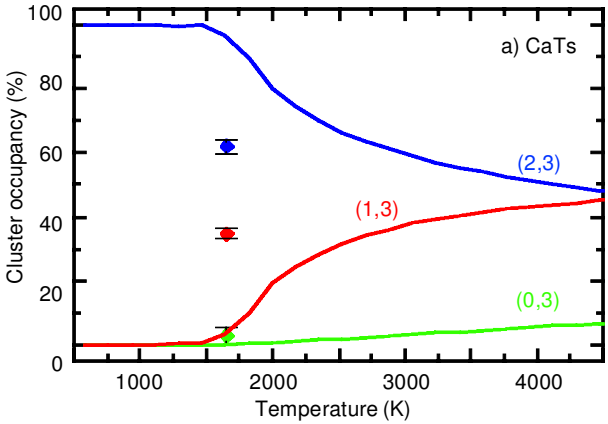
a) CaTs
Cluster occupancy (%)
Temperature (K)
(2,3)
(1,3)
(0,3)

b

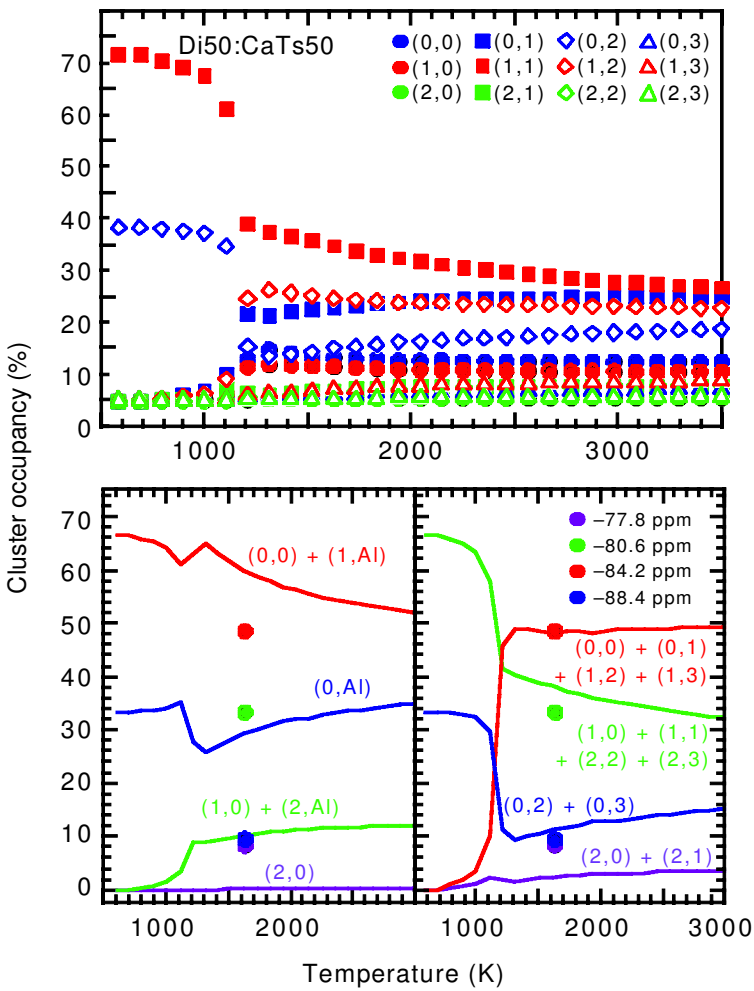
Di50:CaTs50
(0,0) (0,1) (0,2) (0,3)
(1,0) (1,1) (1,2) (1,3)
(2,0) (2,1) (2,2) (2,3)
Cluster occupancy (%)
(0,0) + (1,Al)
(0,Al)
(1,0) + (2,Al)
(2,0)
−77.8 ppm
−80.6 ppm
−84.2 ppm
−88.4 ppm
(0,0) + (0,1) + (1,2) + (1,3)
(1,0) + (1,1) + (2,2) + (2,3)
(0,2) + (0,3)
(2,0) + (2,1)
Temperature (K)

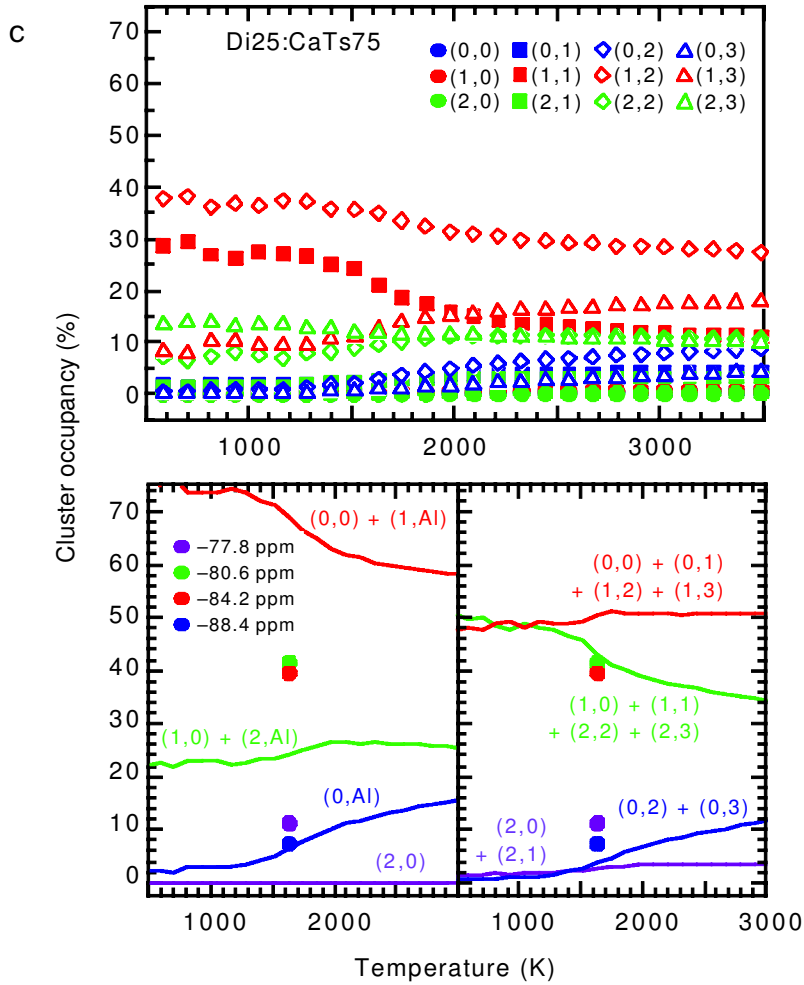

FIG. 12. Calculation of ^{29}Si MAS-NMR peak intensities by MC simulation: (*a*) (*facing page*) the Ca-Tschermak end-member; (*b*) (*facing page*) the Di50:CaTs50 solid solution; and (*c*) the Di25:CaTs75 solid solution. In *b* and *c*, the upper plot shows the temperature dependence of the 9 peaks expected in the spectra; the lower left plot shows the temperature dependence of the 4 combinations of overlapping peaks assumed as the peak assignment by Putnis and Vinograd (1999); and the lower right plot shows a new interpretation based on different combinations of overlapping peaks. All plots show the experimental peak intensities (from Bosenick *et al.*, 1999*b*).

could not be obtained using self-consistency arguments and theoretical considerations alone.

Thermodynamic integration

Background theory

Thermodynamic integration provides a route to obtaining the free energy (and hence also entropy) of ordering from MC simulations. The method is not new, but it is not often documented in its general form, and as far as we are aware it has not been documented in an appropriate form for the type of problem we are considering here. The idea is to start from a model for which the free energy is known exactly, and to work from that solution to the free energy of the model being studied. The important component of the theory is the relation between the free energy F and the partition function. In a discrete formalism, the partition function Z is the sum over all states of the system:

$$Z = \sum_j \exp(-\beta E_j)$$

where $\beta = 1/k_B T$ (as before), and E_j is the energy of the jth state. The energy can be represented by the Hamiltonian for a given state point, in which case we could write the partition function as

$$Z = \frac{\int \exp(-\beta H(\mathbf{q}))\mathrm{d}\mathbf{q}}{\int \mathrm{d}\mathbf{q}} \rightarrow \sum_j \exp\left(-\beta H(\mathbf{q}_j)\right)$$

where $\mathbf{q}$ is the vector of the fundamental variables of the system (such as atom positions), and is either a continuous variable, as in the integral representation, or a discrete variable, as in the summation representation. For any quantity $\varphi(\mathbf{q})$ that depends on the fundamental variables, which we now take to be discrete rather than continuous, the average over all configurations is written as

$$\langle \varphi \rangle = \frac{1}{Z} \sum_j \varphi(\mathbf{q}_j) \exp(-\beta H(\mathbf{q}_j))$$

It is impossible to sum over all configurations, but it is found that the way that MC method samples the phase space of configurations is good enough to give reasonably accurate values of ensemble averages. This statement is proved by the fact that ensemble averages and their standard deviations do not depend on the number of MC steps used in a simulation within the usual limits of statistical noise.

The free energy is related to the partition function by

$$F = -\frac{1}{\beta} \ln Z$$

The problem we face in the calculation of F is that the partition function cannot be computed in a simulation, since, unlike calculations of ensemble averages, it does require calculation of all terms, including those that are of low probability. The calculation of the free energy requires a method that is based on the reliable computation of ensemble averages, and the method of thermodynamic integration provides this possibility.

The method of thermodynamic integration requires a reference point of a model Hamiltonian for which we know the corresponding free energy exactly. We label this model Hamiltonian as H_0, and the corresponding free energy is F_0. We now define the Hamiltonian H_λ as a mixture of the actual and model Hamiltonians:

$$H_\lambda = \lambda H + (1 - \lambda) H_0 = H_0 + \lambda(H - H_0) = H_0 + \lambda \Delta H$$

where λ is the mixing parameter, which varies in value between 0 and 1. The last term defines the difference quantity ΔH, which we will use below. We also note, for reference below, that the differential is simply given as $\partial H_\lambda / \partial \lambda = \Delta H$.

The free energy can be represented by the integral

$$F = F_0 + \int_0^1 \frac{\partial F_\lambda}{\partial \lambda} \mathrm{d}\lambda$$

where F_λ is the free energy corresponding to the Hamiltonian H_λ. This can be written in terms of the partition function:

$$Z_\lambda = \sum_j \exp(-\beta H_\lambda(\mathbf{q}_j))$$

$$F_\lambda = -\frac{1}{\beta} \ln Z_\lambda = -\frac{1}{\beta} \ln \sum_j \exp(-\beta H_\lambda(\mathbf{q}_j))$$

The differential of F_λ with respect to λ follows as

$$\begin{aligned} \frac{\partial F_\lambda}{\partial \lambda} &= -\frac{1}{\beta Z_\lambda} \frac{\partial Z_\lambda}{\partial \lambda} \\ &= \frac{1}{Z_\lambda} \sum_j \frac{\partial H_\lambda(\mathbf{q}_j)}{\partial \lambda} \exp\left(-\beta H_\lambda(\mathbf{q}_j)\right) \\ &= \frac{1}{Z_\lambda} \sum_j \Delta H(\mathbf{q}_j) \exp\left(-\beta H_\lambda(\mathbf{q}_j)\right) \\ &= \langle \Delta H \rangle_\lambda \end{aligned}$$

We have written the last line of this equation explicitly in order to highlight the fact that the differential of F_λ is simply equal to the statistical average value of ΔH calculated from a set of configurations corresponding to the mixed Hamiltonian H_λ. The subscript λ on $\langle \Delta H \rangle_\lambda$ implies that the average is obtained from configurations generated by the Hamiltonian H_λ. Since average quantities can be calculated with reasonable accuracy, we now have a handle on the free energy.

For ordering processes, a good model Hamiltonian is the trivial case of having non-interacting cations, written mathematically as

$$H_0 = 0$$

With this choice of model Hamiltonian, we have

$$H_\lambda = \lambda H; \quad \Delta H = H$$

Hence

$$\frac{\partial F_\lambda}{\partial \lambda} = \langle H \rangle_\lambda$$

This is simply the average energy of a system subject to the Hamiltonian λH. In practice, it means running the simulation with interactions corresponding to the Hamiltonian λH, and then computing the average energy as if the Hamiltonian was really given by H. The energy is calculated using H, but the simulation that produces the configurations is driven by the Hamiltonian λH.

A system with the Hamiltonian $H_0 = 0$ will have complete disorder at all temperatures, and the corresponding free energy F_0 will simply be obtained from the configurational entropy of a system with a random arrangement. If we have several types of atoms on N symmetrically equivalent sites, each with fraction x_j, we have the standard result

$$F_0 = N\beta^{-1}\sum_j x_j \ln x_j$$

Taking together the results for $\partial F_\lambda/\partial\lambda$ and F_0, the free energy is given as

$$F = F_0 + \int_0^1 \langle H\rangle_\lambda \mathrm{d}\lambda$$

The idea then is to perform calculations of the average $\langle H\rangle_\lambda$ for many values of λ and perform a numerical integration. The point is that although the MC simulation does not sample the complete set of configurations, the averages that are used in the integrals can be calculated with sufficient accuracy to enable the free energy to be calculated with reasonable accuracy.

At first sight it appears costly to have to run the simulations at many values of λ in order to determine the free energy at a single temperature. However, it turns out that we can exploit the situation to enable us to calculate the free energy as a function of temperature at no further cost. We noted above that when $H_0 = 0$, $H_\lambda = \lambda H$. Thus a simulation performed with H_λ at temperature T is equivalent to a simulation performed with H at temperature $T_\lambda = T/\lambda$. So if we perform the integration for values of λ between 0 and λ' for a temperature T, instead of between 0 and 1, it is equivalent to performing the integration between 0 and 1 for a temperature equal to $T_{\lambda'} = T/\lambda'$. At higher values of temperature the system is more disordered and the free energy is closer to the value for a random system. Therefore there is less variation for different values of λ, and the number of points needed to get a good numerical integration is smaller. Thus if we run the simulation at a given temperature for many values of λ, we can obtain the free energy as a function of temperature for a wide range of temperatures above the notional temperature of the simulation. Thus we make full use of all the data generated in the simulation. Moreover, for each value of λ we can also calculate other ensemble averages, such as the order parameter or susceptibility, which will correspond to the values at a temperature of T_λ. The only limitation is that for numerical integration over λ it is better to run the separate simulations with equal increments of λ, which means that the resultant analysis will have uniform steps of $1/T$ on the temperature scale.

In the implementation of the method in Ossia99 the MC simulation is run for a predetermined number n_λ of equally-spaced values of λ between $1/n_\lambda$ and 1 for a temperature T. The nth value is equal to $\lambda_n = n/n_\lambda$, and, following the discussion in the previous paragraph, corresponds to a temperature $T_n = T/\lambda_n = n_\lambda T/n$. The MC simulation gives the energy $E_\lambda = \langle H_\lambda\rangle_\lambda$ for simulations performed with the Hamiltonian λH for all values of λ at temperature T. A separate program is used to perform a numerical integration of the values of E_λ/λ, which are equivalent to $\langle H\rangle_\lambda$, for all values of λ to give the free energy for temperature T. For temperature T_n, the numerical integral is performed for values of λ up to λ_n to give the free energy for this temperature.

Finally, we remark that since we have obtained both $E(T)$ and $F(T)$ directly from the MC simulations via the thermodynamic integration, these two quantities can be combined to give the entropy $S(T)$ using the standard thermodynamic relation:

$$S(T) = \frac{E(T) - F(T)}{T}$$

Thus we can obtain a complete description of the thermodynamic properties of a system.

This method was used to study the composition and temperature dependence of the thermodynamic functions for Al/Si ordering on tetrahedral sites of the feldspar structure (Myers *et al.*, 1998). Some validation of the results was provided by the Cluster Variation Method calculations of Vinograd and Putnis (1998, 1999) and Vinograd *et al.* (2001).

Thermodynamics of cation ordering in spinel

From the MC simulations of spinel described earlier, the thermodynamic functions were calculated using thermodynamic integration (Warren *et al.*, 2000*a,b*). These are shown in Fig. 13. The temperature-dependence of the enthalpy is compared with experimental data from Navrotsky and Klappa (1987) in this figure. The baseline values have been adjusted to enable the experimental and theoretical curves to be plotted together (note that the baseline values are not defined on an absolute scale in either case). The important point of comparison between experiment and theory is the changes of energy with temperature, and in this regard the agreement is very good, aside from the highest-temperature datum which does not follow the trend of the other data. In Fig. 13 the entropy is compared with the only experimental datum available, namely an indirect determination at the single temperature of 1000 K based on phase diagram data (Wood *et al.*, 1986). The agreement between this one measurement and the MC results is remarkably good. Taken with the

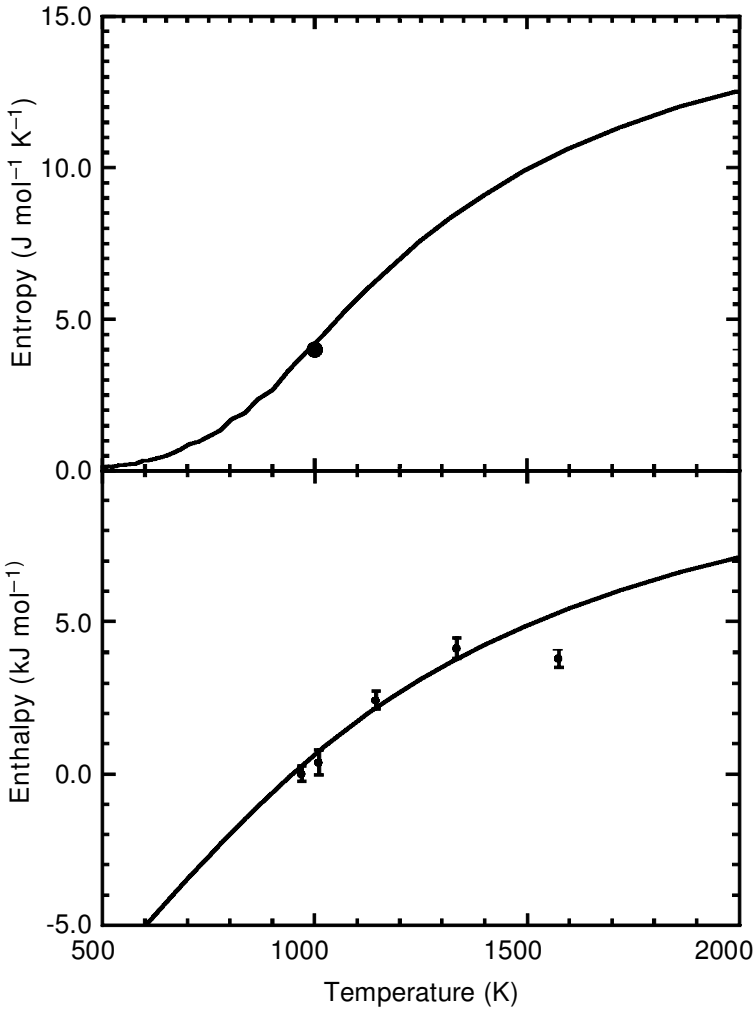

FIG. 13. Thermodynamic functions, entropy and enthalpy, for the Mg/Al ordering process in spinel calculated by MC simulations, compared with the few experimental data available. The experimental data for enthalpy are from Navrotsky and Kleppa (1967), and for entropy from Wood *et al.* (1986).

agreement between the measured and calculated temperature dependence of the order parameter (discussed earlier, Fig. 7), we are able to conclude that the procedure of using a parameterized Hamiltonian that is obtained from *ab initio* quantum mechanical calculations is able to reproduce the experimental behaviour remarkably well. It is important to appreciate that no experimental data were used in any respect in the determination of the model Hamiltonian, in contrast to empirical potentials, which at some stage in their development have been tuned against experimental data. The point, though, is not just that the method gives good agreement with experimental data, but that it can be used to obtain new science insights that cannot be deduced from experiment. We now describe one of these insights.

The temperature-dependence of the free energy and order parameter calculated by the MC simulations were fitted by a classical Landau free energy function appropriate for non-convergent ordering (Carpenter *et al.*, 1994; Carpenter and Salje, 1994; Warren *et al.*, 2000*b*). This resembles the procedure that is often carried out in experimental studies, and was primarily carried out here in order to provide a numerical test of the practice. In particular, we have data for both free energy and order parameter, whereas it is more usual to have experimental data only for the order parameter. The fitting was carried out only for temperatures above a minimum temperature in order to avoid fitting to data where effects due to the second law of thermodynamics not otherwise incorporated into the Landau theory become important. Two values of the minimum temperature were tested. The results are shown in Fig. 14, from which it can be seen that the Landau function (Carpenter *et al.*, 1994; Carpenter and Salje, 1994) provides a very good description of the high-temperature behaviour of the thermodynamics associated with the cation ordering in spinel. It is not common to measure free energies, and free energy functions are usually fitted only to experimental data that depend on some derivative of the free energy. In the present case, we have been able to combine both the free energy and a derivative of the free energy in the fitting of a particular function, and have shown that the Landau description works very well. This provides a justification for fitting experimental measurements of the order parameter to a Landau formalism.

Entropy of the pyrope–grossular solid solution

The entropy associated with variation of the short-range order across the pyrope–grossular solution calculated in the MC simulations is shown in Fig. 15 (Bosenick *et al.*, 2000). For the more dilute solid solutions there is little variation in the entropy with temperature, but for compositions of ~1:1 Mg:Ca the entropy falls considerably on cooling due to the formation of considerable short-range order. It is interesting to compare the scale of the temperature dependence seen in the entropy with that for the calculated MAS-NMR spectra described earlier and shown in Fig. 8. It is clear that the entropy is far more sensitive to the development of short-range ordering than the MAS-NMR results, a feature that is also seen in the pyroxene solid solution (discussed next).

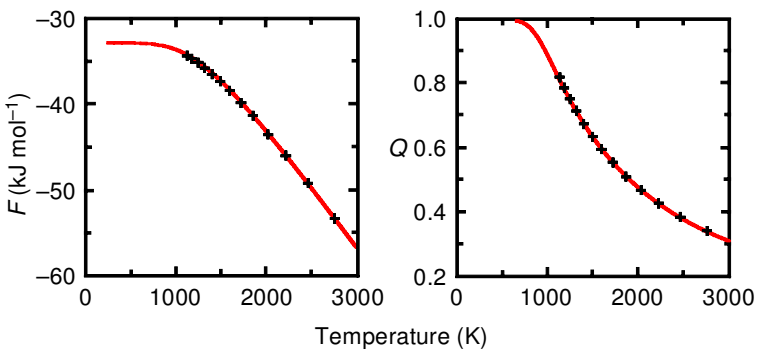

FIG. 14. Free energy and order parameter of spinel calculated by the MC simulations and fitted by a Landau free energy polynomial (after Warren *et al.*, 2000*b*).

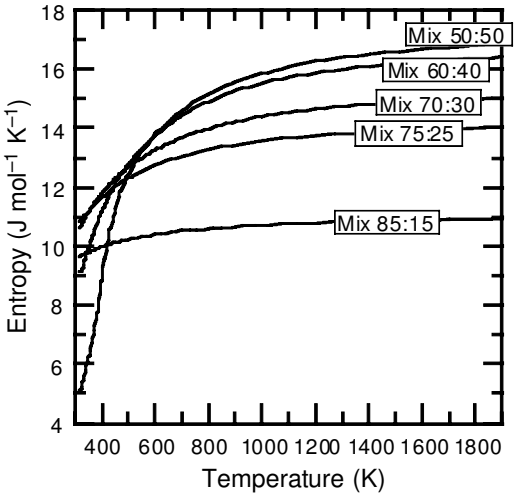

FIG. 15. Temperature dependence of the entropy for members of the pyrope–grossular solid solution calculated by MC simulation (after Bosenick *et al.*, 2000).

Entropy of the diopside–Ca-Tschermak solid solution

Studies of the reaction (Gasparik, 1984)

$$3\ CaAl_2SiO_6 \rightleftharpoons Ca_3Al_2Si_3O_{12} + 2\ Al_2O_3$$
Ca-Tschermack Grossular Corundum

in the temperature range between 1400–1800 K have shown that the configurational entropy of Ca-Tschermak is reduced to ~70% of the random value, S^{ran} = 11.53 J mol^{-1} K^{-1}.

The temperature dependence of the configurational entropy, S, of the end-member Ca-Tschermak calculated in the MC simulations is shown in Fig. 16. Even at temperatures well above the ordering-phase transition temperature, short-range ordering of Si/Al in the tetrahedral sites leads to a strong reduction in the entropy. At a temperature of 2700 K, which corresponds to the temperature where the simulated and observed MAS-NMR intensities of Ca-Tschermak match, the configurational entropy is 7.2 J mol^{-1} K^{-1}. Hence, because of the existence of short-range order, the entropy is reduced to ~65% of the value for a completely random arrangement of Si/Al cations. This is in remarkable agreement with the experimental observation. It is worth noting that the change in the entropy (~35%) from the completely random result is significantly larger than the corresponding change in the MAS-NMR cluster probabilities (~25% at 2700 K). This is similar to the case of the garnet solid solution discussed above.

MC simulations on the solid-solutions Di75:CaTs25 and Di50:CaTs50 also predict strong reductions in the configurational entropies. In these members of the solid solution, the changes in entropy are much more dramatic than the variation in the MAS-NMR cluster occupancies. For example, in Di50:CaTs50 at 2700 K, the reduction in the entropy is 20% from the random value, but the changes in the MAS-NMR cluster occupancies are only 2%. In Di75:CaTs25 at 2700 K, the reduction in the entropy is 15% smaller than the random value, but the variation in the MAS-NMR cluster occupancies are only ~3%. The much lower sensitivity of the MAS-NMR cluster occupancies to short-range ordering than the sensitivity of the entropy implies that it might

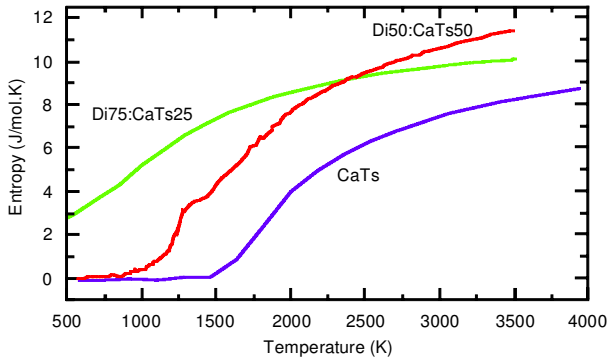

FIG. 16. Temperature dependence of the entropy of members of the diopside:Cs-Tschermak solid solution calculated by the MC simulations.

be difficult to estimate exact entropy values from MAS-NMR peak intensities. This is especially true for cases where MAS-NMR spectroscopy is sensitive to many different cation clusters because to first and second shell interactions, as in the case of pyrope-grossular and diopside–Ca-Tschermak solid-solutions.

Conclusions

We have described an implementation of the MC method that has been optimized for the study of cation ordering in complex minerals, exploiting the potential of parallel computers in the development of the Ossia99 code. The approach is to use a parameterized Hamiltonian that contains pair interactions to any arbitrary distance, but which can also include site-specific chemical potential terms and multi-site terms. Calculations performed on a wide range of systems with different ordering processes have shown that MC simulations are able to give a good representation of experimental data.

We have placed particular emphasis on the ability of MC calculations to give information about short-range order and thermodynamic properties. The short-range order can be measured by MAS-NMR spectroscopy, which gives direct information about the relative probabilities of forming small clusters, and these clusters can easily be calculated in an MC simulation. We have shown, however, that the direct interpretation of MAS-NMR data can be difficult, and the MC simulations have a significant role to play in aiding this interpretation. Moreover, in some cases it is apparent that the MAS-NMR spectra are less sensitive to changes in overall order than the thermodynamic properties. These can be calculated in the MC simulations using the method of thermodynamic integration, which, as we have described in this paper, lends itself to routine applications.

Acknowledgements

This research has been supported by NERC (GR3/10606), the EU (Marie Curie fellowship to AB), the Royal Society (travel support for CISD), and Acciones Integradas (UK/Spain, travel support for CISD and MTD). We are grateful to Julian Gale (Imperial College, London) for assistance, and for providing his GULP code. The quantum mechanics calculations were performed on the parallel computers of the Cambridge High Performance Computing Facility (funded by EPSRC and the University of Cambridge). A thoughtful review by Richard Harrison is greatly appreciated.

References

Bosenick, A., Geiger, C.A., Schaller, T. and Sebald, A. (1995) An ^{29}Si MAS NMR and IR spectroscopic investigation of synthetic pyrope-grossular garnet solid solutions. *Amer. Mineral.*, **80**, 691–704.

Bosenick, A., Dove, M.T., Warren, M.C. and Fisher A. (1999*a*) Local cation distribution of Diopside–Ca-Tschermak solid solutions: A computational and ^{29}Si MAS NMR spectroscopic study. *Eur. J. Mineral.*, **9**, 39.

Bosenick, A., Geiger, C.A. and Phillips, B.L. (1999*b*) Local Ca-Mg distribution of Mg-rich pyrope-grossular garnets synthesized at different temperatures revealed by ^{29}Si MAS NMR spectroscopy. *Amer. Mineral.*, **84**, 1423–33.

Bosenick, A., Dove, M.T. and Geiger, C.A. (2000) Simulation studies of pyrope–grossular solid solutions. *Phys. Chem. Miner.*, **27**, 398–418.

Bosenick, A., Dove, M.T., Myers, E.R., Palin, E.J., Sainz-Diaz, C.I., Guiton, B., Warren, M.C., Craig, M.S. and Redfern, S.A.T. (2001*a*) Computational methods for the study of energies of cation distributions: applications to cation-ordering phase transitions and solid solutions. *Mineral. Mag.*, **65**, 193–219.

Bosenick, A., Dove, M.T., Heine, V. and Geiger, C.A. (2001*b*) Scaling of thermodynamic mixing properties in garnet solid solutions. *Phys. Chem. Miner.* (in press).

Carpenter, M.A. and Salje, E.K.H (1994) Thermodynamics of nonconvergent cation ordering in minerals. 2. Spinels and the ortho-pyroxene solid-solution. *Amer. Mineral.*, **79**, 1068–83

Carpenter, M.A., Powell, R. and Salje, E.K.H. (1994) Thermodynamics of nonconvergent cation ordering in minerals. 1. An alternative approach. *Amer. Mineral.*, **79**, 1053–67.

Circone, S., Navrotsky, A., Kitkpatrick, R.J. and Graham, C.M. (1991) Substitution of $^{[6,4]}$Al in phlogopite: Mica characterization, unit-cell variation, ^{27}Al and ^{29}Si MAS-NMR spectroscopy, and Al-Si distribution in the tetrahedral sheet. *Amer. Mineral.*, **76**, 1485–501.

Dove, M.T. (1999) Order/disorder phenomena in minerals: ordering phase transitions and solid solutions. Pp. 451–75 in: *Microscopic Processes in Minerals* (C.R.A. Catlow and K. Wright, editors). Kluwer, The Netherlands.

Dove, M.T., Thayaparam, S., Heine, V. and Hammonds, K.D. (1996) The phenomenon of low Al/Si ordering

temperatures in aluminosilicate framework structures. *Amer. Mineral.*, **81**, 349–62.

Dove, M.T., Bosenick, A., Myers, E.R., Warren, M.C. and Redfern, S.A.T. (2000) Modelling in relation to cation ordering. *Phase Trans.*, **71**, 205–26.

Gasparik, T. (1984) Experimentally determined stability of clinopyroxene + garnet + corundum in the system CaO-MgO-Al_2O_3-SiO_2. *Amer. Mineral.*, **69**, 1025–35.

Herrero, C.P. and Sanz, J. (1991) Short-range order of the Si,Al distribution in layer silicates. *J. Phys. Chem. Solids*, **52**, 1129–35.

Herrero, C.P., Sanz, J. and Serratosa, J.M. (1985) Tetrahedral cation ordering in layer silicates by ^{29}Si NMR spectroscopy. *Solid State Comm.*, **53**, 151–4.

Herrero, C.P., Sanz, J. and Serratosa, J.M. (1986) The electrostatic enery of micas as a function of Si, Al tetrahedral ordering. *J. Physics: Cond. Matter*, **19**, 4169–81.

Herrero, C.P., Gregorkiewitz, M., Sanz, J. and Serratosa, J.M. (1987) Si-29 MAS-NMR spectroscopy of mica-type silicates - observed and predicted distribution of tetrahedral Al-Si. *Phys. Chem. Miner.*, **15**, 84–90.

Herrero, C.P., Sanz, J. and Serratosa, J.M. (1989) Dispersion of charge deficits in the tetrahedral sheet of phyllosilicates. Analysis from ^{29}Si NMR spectra. *J. Phys. Chem.*, **93**, 4311–5.

Millard, R.L. and Luth, R.W. (1998) Tetrahedral Si/Al distribution in Di-CaTs clinopyroxenes using ^{29}Si MAS NMR. *EOS Trans. Amer. Geophys. Union*, **79**, S162.

Myers, E.R., Heine, V. and Dove, M.T. (1998) Thermodynamics of Al/Al avoidance in the ordering of Al/Si tetrahedral framework structures. *Phys. Chem. Miner.*, **25**, 457–64.

Navrotsky, A. and Kleppa, O.J. (1967) The thermodynamics of cation distributions in simple spinels. *J. Inorg. Nucl. Chem.*, **29**, 2701–14.

Okamura, F.P., Ghose, S. and Ohashi, H. (1974) Structure and crystal chemistry of Calcium Tschermak's pyroxene, $CaAlAlSiO_6$. *Amer. Mineral.*, **59**, 549–57.

Palin, E.J., Dove, M.T., Redfern, S.A.T, Bosenick, A., Sainz-Diaz, C.I. and Warren, M.C. (2001) Computational study of tetrahedral Al-Si ordering in muscovite. *Phys. Chem. Miner.* (in press).

Putnis, A. and Vinograd, V. (1999) Principles of solid state NMR spectroscopy and applications to determining local order in minerals. Pp. 389–425 in: *Microscopic Processes in Minerals* (C.R.A. Catlow and K. Wright, editors). Kluwer, The Netherlands.

Putnis, A., Fyfe, C.A. and Gobbi, G.C. (1985) Al,Si ordering in cordierite using magic angle spinning NMR. 1. Si-29 spectra of synthetic cordierites. *Phys. Chem. Miner.*, **12**, 211–6.

Redfern, S.A.T., Harrison, R.J., O'Neill, H.St.C. and Wood, D.R.R. (1999) Thermodynamics and kinetics of ordering in $MgAl_2O_4$ spinel from 1600°C from in situ neutron diffraction *Amer. Mineral.*, **84**, 299–310.

Thayaparam, S., Dove, M.T. and Heine, V. (1994) A computer simulation study of Al/Si ordering in gehlenite and the paradox of the low transition temperature. *Phys. Chem. Miner.*, **21**, 110–6.

Thayaparam, S., Heine, V., Dove, M.T. and Hammonds, K.D. (1996) A computational study of Al/Si ordering in cordierite. *Phys. Chem. Miner.*, **23**, 127–39.

Vinograd, V.L. and Putnis, A. (1998) Calculation of the configurational entropy of Al, Si in layer silicates using the cluster variation method. *Phys. Chem. Miner.*, **26**, 135–48.

Vinograd, V.L. and Putnis, A. (1999) The description of Al, Si ordering in aluminosilicates using the cluster variation method. *Amer. Mineral.*, **84**, 311–24.

Vinograd, V.L., Putnis, A. and Kroll, H. (2001) Structural discontinuities in plagioclase and constraints on mixing properties of the low series: A computational study. *Mineral. Mag.*, **65**, 1–32.

Warren, M.C., Dove, M.T. and Redfern, S.A.T. (2000*a*) *Ab initio* simulations of cation ordering in oxides: application to spinel. *J. Phys.: Cond. Matter*, **12**, L43–8.

Warren, M.C., Dove, M.T. and Redfern, S.A.T. (2000*b*) Disordering of $MgAl_2O_4$ spinel from first principles. *Mineral. Mag.*, **64**, 311–7.

Wood, B.J., Kirkpatrick, R.J. and Montez, B. (1986) Order-disorder phenomena in $MgAl_2O_4$ spinel *Amer. Mineral.*, **71**, 999–1006.

Yeomans, J.M. (1992) *Statistical Mechanics of Phase Transitions*. Oxford University Press, New York.

[*Manuscript received 15 September 2000: revised 7 December 2000*]